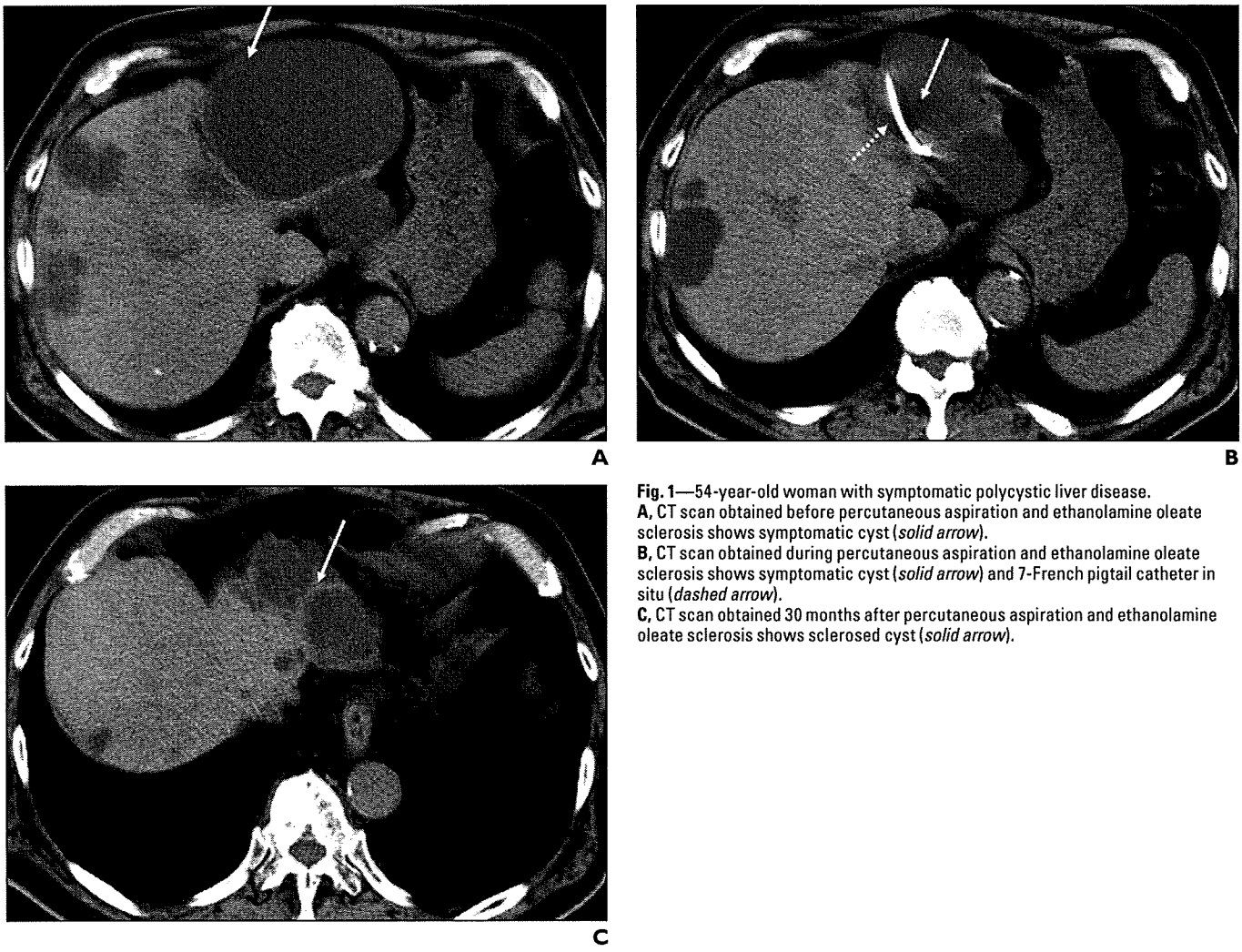

Fig. 1—54-year-old woman with symptomatic polycystic liver disease.
A, CT scan obtained before percutaneous aspiration and ethanolamine oleate sclerosis shows symptomatic cyst (*solid arrow*).
B, CT scan obtained during percutaneous aspiration and ethanolamine oleate sclerosis shows symptomatic cyst (*solid arrow*) and 7-French pigtail catheter in situ (*dashed arrow*).
C, CT scan obtained 30 months after percutaneous aspiration and ethanolamine oleate sclerosis shows sclerosed cyst (*solid arrow*).

etate in the blood stream. Thus persons with congenital acetaldehyde dehydrogenase deficiency are at greater risk of prolonged hypotension than those with normal levels of this enzyme. One of the late complications of ethanol sclerosis has been intracystic hemorrhage [21]. Therefore, in comparison with ethanol sclerosis, ethanolamine oleate sclerosis not only achieves much better reduction without recurrence or need for surgery but also has a more favorable short-term and long-term adverse effect profile.

Surgical therapy has been the mainstay of management of PLD. Open and laparoscopic fenestration procedures, which are the least invasive surgical procedures, have recurrence rates of 11–100% and 0–100%, respectively, and morbidity rates of 0–66% and 0–67% [5, 20, 24–26]. The rate of symptom recurrence for laparotomy with fenestration ranged from 11% to 26% in the largest case series [20]. The combination of fenestration and hepatic resection has a low mortality (3–11%) but relatively high morbidity rate (20–100%) and can be considered only for patients with extreme symptoms [20, 27, 28]. Liver transplantation, the most invasive of techniques, is indicated in the care of patients with symptoms refractory to other techniques or who have liver disease combined with renal failure [29]. Experience with hepatic arterial embolization for PLD is limited to a single published report [30] and hepatic arterial embolization is a more invasive technique than percutaneous aspiration and sclerosis and cannot be directed at a specific cyst.

Limitations of this study were the small number of patients, that it was conducted at a single center, that patient inclusion was not randomized, and lack of a control arm. In addition, follow-up data collection varied widely; data on only 47.1% (8/17) and 35% of the cysts were available 3 months and 1 year after treatment. We conclude that a single session of percutaneous aspiration and ethanolamine oleate sclerosis is safe and effective, resulting in sustained resolution for a long follow-up period with minimal morbidity and preventing surgery. Further randomized control trials and comparison with existing surgical and nonsurgical options are needed.

References

1. Erdogan D, van Delden OM, Rauws EA, et al. Results of percutaneous sclerotherapy and surgical treatment in patients with symptomatic simple liver cysts and polycystic liver disease. *World J Gastroenterol* 2007; 13:3095–3100
2. Regev A, Reddy KR. Benign solid and cystic tumors of the liver. In: Reddy KR, Long WB, eds. *Hepatobiliary tract and pancreas.* Edinburgh, UK: Mosby, 2004: 189–214

3. Takei R, Ubara Y, Hosino J, et al. Percutaneous transcatheter hepatic artery embolization for liver cysts in autosomal dominant polycystic kidney disease. *Am J Kidney Dis* 2007; 49:744–752
4. Saini S, Mueller PR, Ferrucci JT Jr, et al. Percutaneous aspiration of hepatic cysts does not provide definitive therapy. *AJR* 1983; 141:559–560
5. Koperna T, Vogl S, Satzinger U, et al. Nonparasitic cysts of the liver: results and options of surgical treatment. *World J Surg* 1997; 21:850–854
6. Montorsi M, Torzilli G, Fumagalli U, et al. Percutaneous alcohol sclerotherapy of simple hepatic cysts: results from a multicentre survey in Italy. *HPB Surg* 1994; 8:89–94
7. Bean WJ, Rodan BA. Hepatic cysts: treatment with alcohol. *AJR* 1985; 144:237–241
8. Gelczer RK, Charboneau W, Hussain S, et al. Complications of percutaneous ethanol ablation. *J Ultrasound Med* 1998; 17:531–533
9. Goldstein HM, Carlyle DR, Nelson RS. Treatment of symptomatic hepatic cyst by percutaneous instillation of Pantopaque. *AJR* 1976; 127:850–853
10. Davies CW, McIntyre AS. Treatment of a symptomatic hepatic cyst by tetracycline hydrochloride instillation sclerosis. *Eur J Gastroenterol Hepatol* 1996; 8:173–175
11. vanSonnenberg E, Wroblicka JT, D'Agostino HB, et al. Symptomatic hepatic cysts: percutaneous drainage and sclerosis. *Radiology* 1994; 190:387–392
12. Kasahara A, Hayashi N, Kono M, et al. Successful treatment of a hepatic cyst by one-shot instillation of minocycline chloride. *Gastroenterology* 1992; 103:675–677
13. Sanchez H, Gagner M, Rossi RL, et al. Surgical management of nonparasitic cystic liver disease. *Am J Surg* 1991; 161:113–118
14. Torres VE. Treatment of polycystic liver disease: one size does not fit all. *Am J Kidney Dis* 2007; 49:725–728
15. Iso Y, Kitano S, Iwanaga T, et al. A prospective randomized study comparing the effects of large and small volumes of the sclerosant 5% ethanolamine oleate injected into esophageal varices. *Endoscopy* 1988; 20:285–288
16. Orikasa K. Studies on the damage of the cultured endothelial cells and K-562 cells by sclerosants used for treatment of esophageal varices [in Japanese]. *Nippon Shokakibyo Gakkai Zasshi* 1989; 86:2365–2372
17. Yamamoto K, Sakaguchi H, Anai H, et al. Sclerotherapy for simple cysts with use of ethanolamine oleate: preliminary experience. *Cardiovasc Intervent Radiol* 2005; 28:751–755
18. Mortele KJ, Ros PR. Cystic focal liver lesions in the adult: differential CT and MR imaging features. *RadioGraphics* 2001; 21:895–910
19. Trinkl W, Sassaris M, Hunter FM. Nonsurgical treatment for symptomatic nonparasitic liver cysts. *Am J Gastroenterol* 1985; 80:907–911
20. Arnold HL, Harrison SA. New Advances in evaluation and management of patients with polycystic liver disease. *Am J Gastroenterol* 2005; 100: 2569–2582
21. Akinci D, Akhan O, Ozmen M, et al. Long-term results of single-session percutaneous drainage and ethanol sclerotherapy in simple renal cysts. *Eur J Radiol* 2005; 54:298–302
22. Spiegel RM, King DL, Green WM. Ultrasonography of primary cysts of the liver. *AJR* 1978; 131: 235–238
23. Kairaluoma MI, Leinonen A, Ståhlberg M, et al. Percutaneous aspiration and alcohol sclerotherapy for symptomatic hepatic cysts: an alternative to surgical intervention. *Ann Surg* 1989; 210:208–215
24. Tan YM, Chung A, Mack P, et al. Role of fenestration and resection for symptomatic solitary liver cysts. *ANZ J Surg* 2005; 75:577–580
25. Fiamingo P, Tedeschi U, Veroux M, et al. Laparoscopic treatment of simple hepatic cysts and polycystic liver disease. *Surg Endosc* 2003; 17:623–626
26. Yang GS, Li QG, Lu JH, et al. Combined hepatic resection with fenestration for highly symptomatic polycystic liver disease: a report on seven patients. *World J Gastroenterol* 2004; 10:2598–2601
27. Tan YM, Ooi LL. Highly symptomatic adult polycystic liver disease: options and results of surgical management. *ANZ J Surg* 2004; 74:653–657
28. Kornprat P, Cerwenka H, Bacher H, et al. Surgical therapy options in polycystic liver disease. *Wien Klin Wochenschr* 2005; 117:215–218
29. Garcea G, Pattenden CJ, Stephenson J, et al. Nine-year single-center experience with nonparasitic liver cysts: diagnosis and management. *Dig Dis Sci* 2007; 52:185–191
30. Takei R, Ubara Y, Hoshino J, et al. Percutaneous transcatheter hepatic artery embolization for liver cysts in autosomal dominant polycystic kidney disease. *Am J Kidney Dis* 2007; 49:744–752

J Gastroenterol 2009; 44[Suppl XIX]:112–118
DOI 10.1007/s00535-008-2274-6

Journal of Gastroenterology

Multistep human hepatocarcinogenesis: correlation of imaging with pathology

Masatoshi Kudo

Department of Gastroenterology and Hepatology, Kinki University School of Medicine, 377-2 Ohno-Higashi, Osaka-Sayama 589-8511, Japan

Hepatocellular carcinoma (HCC) is one of the most common malignancies worldwide. The majority of HCCs develop in cirrhotic livers, and the early detection and characterization of this entity is very important. Pathologically, human HCC develops in a multistep fashion in the following sequence: from low-grade dysplastic nodule (LGDN), to high-grade dysplastic nodule (HGDN), early HCC, well-differentiated HCC, nodule-in-nodule HCC, and, finally, to moderately differentiated HCC. Differentiation between early HCC and DN is the most important issue in the clinical setting. CT during hepatic angiography (CTHA) and CT during arterial portography (CTAP) are the most sensitive tools in the differentiation of premalignant/borderline lesions (LGDN and HGDN) and early HCC. Recent progress in imaging modality, especially Sonazoid-enhanced US and Gd-EOB-DTPA MRI, is starting to play a very important role in the imaging of multistep hepatocarcinogenesis, resulting in changing the therapeutic strategy of these nodular lesions associated with liver cirrhosis.

Key words: hepatocellular carcinoma, low grade dysplastic nodule, high grade dysplastic nodule, early HCC, nodule-in-nodule HCC

Introduction

Hepatocellular carcinoma (HCC) is one of the most common malignancies worldwide. The majority of HCCs develop in cirrhotic livers, and the early detection and characterization of this entity is very important for the management of patients with cirrhosis. In Japan, more than 90% of HCCs are associated with hepatitis B or C virus infection, 80% of them with hepatitis C. This intense epidemiological relationship between hepatitis B or C and HCC suggests the carcinogenic role of these viruses.[1,2] The development of screening programs for high-risk HCC patients with periodic ultrasonography (US), computed tomography (CT), and measurement of tumor markers (AFP, PIVKA-II, AFP-L3) has enabled small HCCs of less than 2 cm to be easily detected and safely resected. As a result, we have encountered more early-stage HCCs than classical advanced HCCs, including early HCC, low-grade dysplastic nodules (LGDNs), and high-grade dysplastic nodules (HGDNs).[3–5] The majority of these lesions are hypovascular upon dynamic CT or angiography.[6] Therefore, the enhancement pattern of these lesions upon dynamic CT is notably different from that of overt HCC.[6–12] The intensity of early HCC on T_1- and T_2-weighted MR images is also different from that of overt HCC.[13,14]

Until early-stage HCC was pathologically and clinically identified, most radiologists and hepatologists believed that HCC was generally hypervascular upon angiography and/or dynamic CT, except for a few cases with spontaneous necrosis or well-differentiated HCC.[15]

Received: June 10, 2008 / Accepted: August 2, 2008
Reprint requests to: M. Kudo

Classification of hepatocellular nodules

The nodules associated with liver cirrhosis are histologically divided into six categories according to the classification proposed by the Liver Cancer Study Group of Japan:[16] large regenerative nodules, adenomatous hyperplasia (AH), atypical AH, early HCC, well-differentiated HCC, and moderately or poorly differentiated HCC (so-called classical HCC). On the other hand, the International Working Party of the World Congress of Gastroenterology[17] proposed a new classification in 1995. According to the new classification,

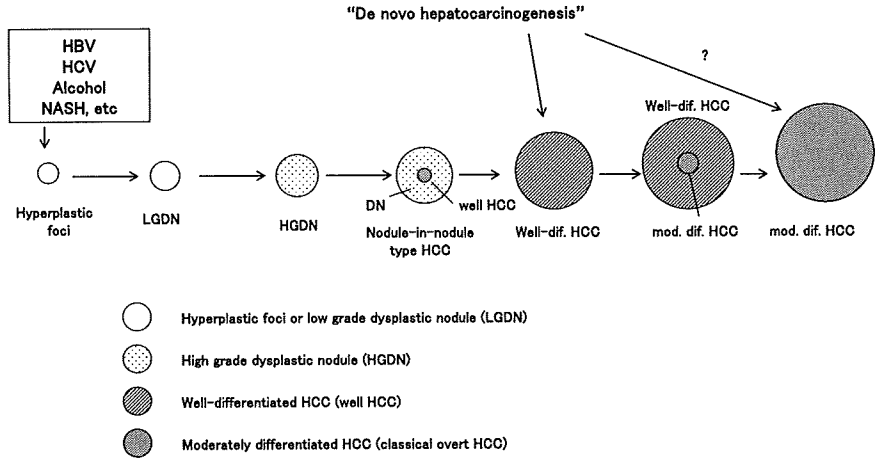

Fig. 1. Schematic representation of multistep progression of human hepatocarcinogenesis

hepatocellular nodules are divided into two categories, namely, dysplastic nodules (DNs) and HCC. DNs are defined as dysplastic nodules of hepatocytes at least 1 mm in diameter, with dysplasia but without histological criteria of malignancy, and are divided into two subtypes. The first subtype is LGDN, i.e., a nodule in which atypia is mild. These nodules are composed of hepatocytes that are minimally abnormal. The nuclear-to-cytoplasmic ratio is normal or slightly increased. Portal tracts are present. The second subtype is HGDN, i.e., a nodule in which atypia is at least moderate but insufficient for diagnosis of malignancy. One or more of the following may be seen: high nuclear-to-cytoplasmic ratio, nuclear hyperchromasia, plates more than two cells wide, pseudoglandular formation, and cytoplasmic basophilia. Invasion into stroma or portal tracts is absent. On the other hand, HCC is defined as a malignant neoplasm composed of cells with hepatocellular differentiation. LGDNs are considered to be consistent with a large regenerative nodule or AH, and HGDNs with atypical AH and some early HCCs. HGDNs are considered neoplastic because they display variable atypical changes in hepatocytes and have increased cell proliferation.[17,18] It is of interest that cancerous foci of very well differentiated HCC are occasionally encountered within this type of nodule (nodule-in-nodule lesions), called a DN with a subfocus of HCC. On the other hand, the histopathological definition, identification, and significance of LGDNs remain unclear in routine clinical practice. These nodules can be included in the group of regenerative nodules with unusual histological changes.[18] In these nodules, two types of human hepatocarcinogenesis are now considered. One is de novo hepatocarcinogenesis, and the other is stepwise development from LGDN to HGDN, with well-differentiated HCC foci, and finally to overt HCC[3,5,19–22] (Fig. 1).

The detection and characterization of HCC is one of the major roles of diagnostic imaging in patients with cirrhosis in endemic areas. The differential diagnosis between HCC and other types of nodules is important clinically. However, definite differentiation among these nodules by ultrasound and dynamic CT is usually impossible. For this reason, percutaneous biopsy by ultrasound guidance is frequently performed. However, it is occasionally difficult to obtain an exact tissue sample from these small nodules, and, as recently described by Bhattacharya et al.[23] and Mion et al.[24] using explanted cirrhotic livers, many multicentric small HCCs or borderline lesions are not detected by ultrasound. In addition, several difficulties and controversies remain regarding the differential diagnosis of such nodules in needle biopsy specimens. First, limited information from insufficient small specimens and sampling errors caused by histological heterogeneity within these nodules may lead to under- or overdiagnosis. Second, regenerative reactive hepatocellular atypia in chronic disease resembles atypical changes in DNs or well-differentiated HCCs.[18] Therefore, differential diagnosis by imaging is also important. For this reason, it is clinically useful to visualize by imaging the sequential changes in the intranodular blood supply, in parallel with the progression of benign hepatocellular nodules to overt HCC.

Definition of early HCC (small well-differentiated HCC of vaguely nodular type HCC)

The tumors are vaguely nodular and are characterized by various combinations of the following five major histological features:[7,25,26] (1) increased cell density, more than twice that of the surrounding tissue, with an increased nuclear:cytoplasm ratio and irregular thin trabecular pattern; (2) various numbers of portal tracts within the nodule (intratumoral portal tracts); (3) frequent acinar and/or pseudoglandular pattern; (4) frequent diffuse fatty changes; and (5) varying numbers of

unpaired arteries. Among these features, diffuse fatty change is observed in ~40% of tumors <2 cm in diameter.[27] The prevalence of fatty change decreases along with an increase in tumor size, and fatty change is uncommon in tumors >3 cm and/or moderately differentiated HCCs. Any of these features may be diffuse throughout the lesion or seen in a restricted, usually expansile subnodular (nodule-in-nodule) lesion. Most importantly, because all these features may also be found in HGDNs, it is important to note that some degree of stromal invasion is most helpful in differentiating early HCC from HGDNs.

Multistep progression of hepatocarcinogenesis

Clinical and pathological studies have revealed multistep progression of hepatocarcinogenesis, with increased tumor size form LGDNs to early HCC, through nodule-in-nodule type HCC, and finally to overt HCC[5,22] (see Fig. 1). Although early HCCs are usually <2 cm in diameter, unusual early HCCs and nodule-in-nodule-type HCCs measuring 5 cm have been encountered.[28,29] De novo hepatocarcinogenesis is also presumed to occur as an alternative pathway. Even in such cases, later progression to classical overt HCC takes place in a multistep fashion.

Imaging characteristics of early HCC

Most well-differentiated HCCs at an early stage do not stain upon angiography or retain lipiodol within the tumor, thereby making their diagnosis difficult.[5,6,11,14,30–35] It is widely known that some well-differentiated early-stage HCCs are fed by the portal vein and not by the hepatic artery, in contrast to typical HCCs (Fig. 2).[10,29,36–39] Therefore, some hypovascular HCCs (early HCCs) show no perfusion defects on CT during arterial portography (CTAP) and may look like benign nodules with "benign-appearing" patterns of vasculature.[29]

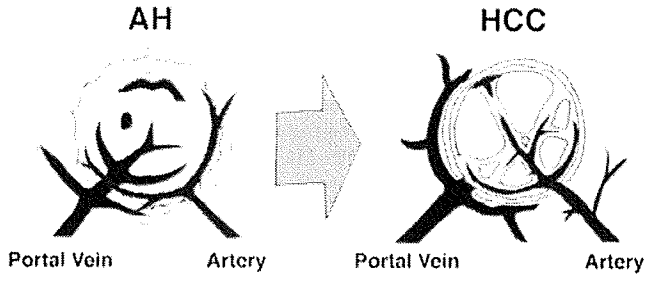

Fig. 2. Schematic representation of blood supplies shifting from LGDN to hepatocellular carcinoma (*HCC*). *AH*, adenomatous hyperplasia

Color Doppler imaging also picks up afferent portal flow signals.[40,41] With the exception of nodules that have a "benign-appearing" hemodynamic pattern, diagnosis of HCC is possible, even at an early stage, by a combined use of tomographic vascular imaging, including US angiography, CT during hepatic angiography (CTHA), and CTAP.[9,10,29,36,37,42,43] Recent progress in contrast-enhanced US has also made it possible to characterize tumor hemodynamics, i.e., separate analysis of arterial and portal supply by using pure arterial-phase imaging.[44]

Progression of hemodynamic and pathological change during multistep human hepatocarcinogenesis

Hepatocarcinogenesis is a multistep process that evolves from hyperplastic nodules (LGDNs) through early HCC, and eventually leads to advanced overt hypervascular HCC.[9,14,22,45] During this process, changes in intranodular hemodynamics occur, which are visualized by their associated radiologic and histopathological findings, as described previously.[29] In the initial phase of carcinogenesis, the hemodynamic pattern shows arterial hypovascularity with portal perfusion still present (type I). In the next step, both arterial and portal blood supplies decrease (type II). Subsequently, intranodular arterial vascularity increases to an isovascular pattern (type III), and finally to a hypervascular pattern (type IV). Another hemodynamic transition occurs from type I to type V (nodule-in-nodule type), which have partial spots of arterial vascularity in a hypovascular background of portal perfusion[8,29,46,47] (Fig. 3).

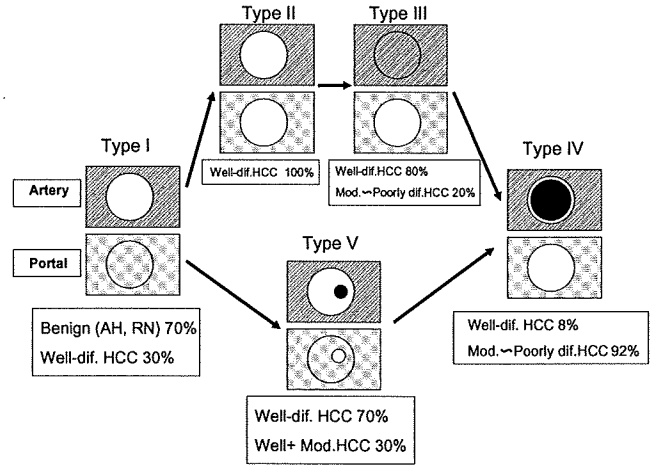

Fig. 3. Schematic representation from premalignant lesion (type I) to well-differentiated HCC (type II and III), nodule-in-nodule type HCC (type V), and to classical overt HCC (type IV). *RN*, regenerative nodule

Fatty metamorphosis is frequently observed in nodules that are hemodynamically classified into types II and III. This appearance is attributed to a relative decrease in the blood supply caused by diminished portal supply and immature arterial neovascularization.[9] Decreased arterial and portal supplies are supported by pathological evidence for decreased density of arterial and portal vessels in well-differentiated early-stage HCC.[27]

When arterial vascularity is observed within the nodule (type III, IV, and V), treatment intervention should be considered according to the treatment algorithm of HCC.[48]

Diagnostic algorithm of premalignant/borderline lesions and early HCC

Among nodular lesions associated with liver cirrhosis, various nodules, such as LGDNs, which are considered to be precancerous lesions, HGDNs, early HCC, and nodule-in-nodule liver cancer, are included as hypovascular nodules.[5,49,50] Regarding the diagnostic and treatment algorithm for such nodules, particularly imaging of hypovascular nodules, the generally accepted procedure is outlined below.

The most sensitive modality capable of objectively depicting the early carcinogenesis process among currently available imaging systems is (1) CTAP, followed by (2) CTHA,[51,52] (3) contrast-enhanced US,[8,53,54] and (4) superparamagnetic iron oxide enhanced-magnetic resonance imaging (SPIO-MRI)[55,56] (Fig. 4). Portal blood flow may be maintained in some cases of DN and early HCC, but reduced in other nodules, even though the pathology remains similar to that of early HCC, in which arterial blood flow has not yet increased. CTAP may sharply detect the earliest initial change in HCC. The second earliest initial carcinogenic change is detected as an increase in intranodular arterial blood flow by CTHA or contrast-enhanced US. Hypervascular lesions depicted as nodule-in-nodule or as entirely hypervascular can be interpreted as advanced cancer, even though they are small, which might have already reached a more advanced stage than early liver cancer.

There are variations among cases regarding whether SPIO-MRI or CTHA detects the initial malignant or cancerous changes earlier. Some hypervascular, well-differentiated liver cancer nodules may uptake SPIO on MRI, but reduced uptake has already started in some hypovascular tumor nodules. Therefore, generalization of findings occurring earlier in carcinogenesis remains difficult, i.e., sinusoidal capillarization and the number of Kupffer cells are somewhat dissociated in some cases.

Multidetector raw CT (MDCT) and dynamic MRI are sensitive for detection of arterial blood flow, but are incapable of detecting arterial vascularity in some nodules, depending on the acquisition time, tumor location, and liver function, although the lesions are hypervascular on CTHA and contrast-enhanced US. Nodules intensely enhanced on MDCT and dynamic MRI can be assumed to already exhibit high intensity upon T_2-weighted MRI[57] (Fig. 5).

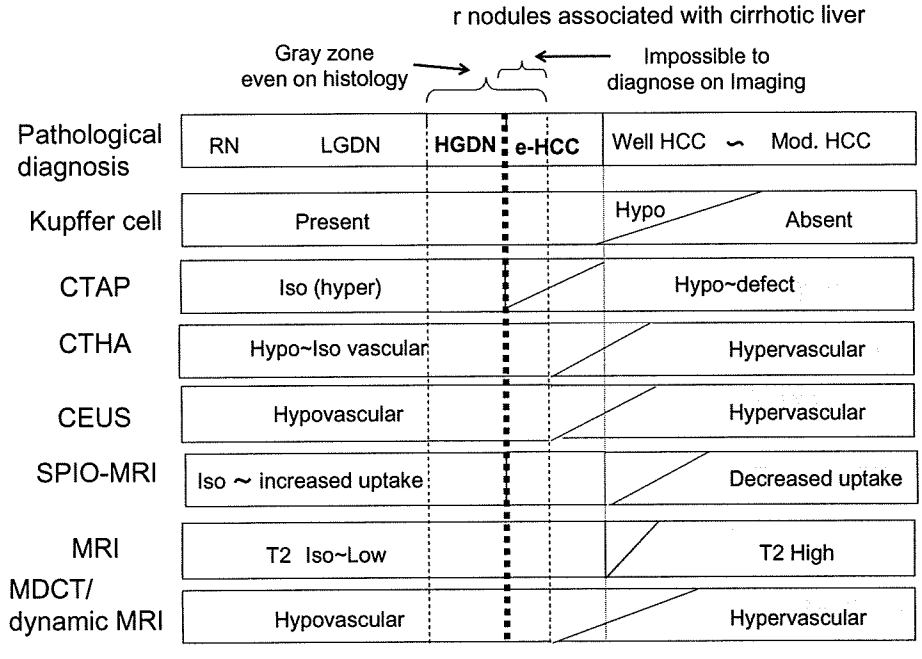

Fig. 4. Imaging findings of hepatocellular nodules associated with cirrhotic liver. *LGDN*, low-grade dysplastic nodule; *HGDN*, high-grade dysplastic nodule; *eHCC*, early HCC; *Well-dif. HCC*, well-differentiated HCC; *Mod. Dif. HCC*, moderately differentiated HCC; *CTAP*, CT during arterial portography; *CTHA*, CT during hepatic arteriography; *CEUS*, contrast-enhanced ultrasonography; *SPIO-MRI*, superparamagnetic iron oxide-enhanced magnetic resonance imaging

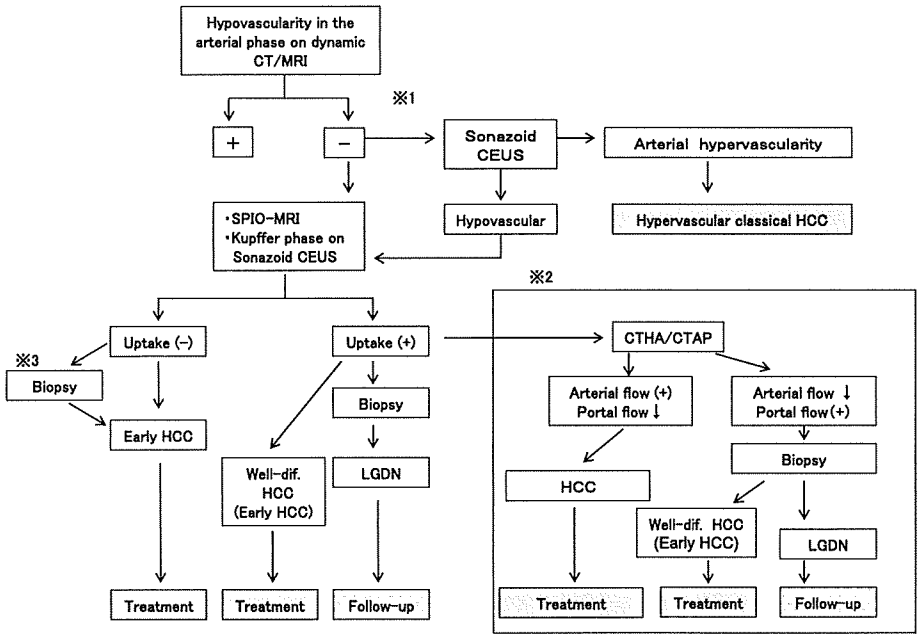

Fig. 5. Diagnostic and treatment algorithm for hypovascular liver nodules. **1:* When the nodule is hypovascular upon dynamic CT or dynamic MRI, Sonazoid-enhanced US is recommended to confirm whether it is actually a hypovascular nodule. **2:* Recommended only at available institutions. **3:* Biopsy is not always necessary in this setting

Based on these observations, lesions detected as hypovascular nodules by MDCT and dynamic MRI should be subjected to Sonazoid-enhanced US (contrast-enhanced US, CEUS) and SPIO-MRI in the diagnostic algorithm for nodules. Sonazoid CEUS is more sensitive for detecting arterial vascularity of target nodules than dynamic CT and dynamic MRI. Thus, hypovascular nodules upon dynamic CT may be diagnosed as hypervascular by CEUS. When uptake of contrast agent by Kupffer cells is reduced in the Kupffer phase of SPIO-MRI and Sonazoid CEUS, malignancy should be highly suspected. Even though uptake of SPIO is noted upon SPIO-MRI, arterial blood flow may be increased in CTHA in some cases. When CTHA/CTAP is not performed or is not available, such nodules should be biopsied. When arterial blood flow is reduced on CTAP, the nodules should be basically regarded and managed as malignant. For nodules with hypovascular arterial blood flow and reduced portal blood flow, biopsy is essential (see Fig. 5).

When Sonazoid is used for CEUS, the combination with MDCT increases the accuracy of detecting intranodular arterial vascularity, compared to that by a single method. Addition of the post-vascular (Kupffer) phase allows an assumption of the degree of malignancy based on Kupffer function. When uptake of contrast agent is reduced in the Kupffer phase of SPIO-MRI or Sonazoid CEUS in nodules not depicted as hypervascular lesions by MDCT or dynamic MRI, the nodules should basically be treated and a biopsy is not essential.

When uptake of SPIO is noted by SPIO-MRI, biopsy should be performed if at all possible, and when diagnosed as typical well-differentiated HCC, the lesions should be treated. When SPIO-MRI detects uptake of SPIO, and CTHA or CTAP detects a malignant finding, i.e., increased arterial blood flow or reduced portal blood flow, the lesions should be regarded as malignant. However, when hypovascular arterial blood flow is noted while the portal blood flow is isovascular, a biopsy is necessary. Nodules histologically diagnosed as benign lesions by biopsy may be subjected to observation without any treatment, but those histologically diagnosed as typical well-differentiated HCC by biopsy should be treated as early HCC.

When CTHA and CTAP are not performed for nodules detected by SPIO-MRI, nodules diagnosed as LGDNs by biopsy may be subjected to observation without any treatment.

Conclusions

In this review, diagnostic imaging of premalignant/borderline lesions and early HCC is described. At present, CTHA and CTAP are the most sensitive imaging modalities for differentiating these lesions, although there are some false-positive results. In addition to MDCT and SPIO-MRI, recently introduced imaging modalities, Sonazoid-enhanced US, and Gadolinium-EthOxyBenzyl-Diethylene-Triamine-Pentaacetic Acid (Gd-EOB-DTPA)-enhanced MRI are the promising tools, which may change the diagnostic strategy in this field.

References

1. Kiyosawa K, Umemura T, Ichijo T, Matsumoto A, Yoshizawa K, Gad A, et al. Hepatocellular carcinoma: recent trends in Japan. Gastroenterology 2004;127:S17–26.
2. Shiratori Y, Shiina S, Imamura M, Kato N, Kanai F, Okudaira T, et al. Characteristic difference of hepatocellular carcinoma between hepatitis B- and C- viral infection in Japan. Hepatology 1995;22:1027–33.
3. Arakawa M, Kage M, Sugihara S, Nakashima T, Suenaga M, Okuda K. Emergence of malignant lesions within an adenomatous hyperplastic nodule in a cirrhotic liver. Observations in five cases. Gastroenterology 1986;91:198–208.
4. Kanai T, Hirohashi S, Upton MP, Noguchi M, Kishi K, Makuuchi M, et al. Pathology of small hepatocellular carcinoma. A proposal for a new gross classification. Cancer (Phila) 1987;60:810–9.
5. Sakamoto M, Hirohashi S, Shimosato Y. Early stages of multistep hepatocarcinogenesis: adenomatous hyperplasia and early hepatocellular carcinoma. Hum Pathol 1991;22:172–8.
6. Krinsky G. Imaging of dysplastic nodules and small hepatocellular carcinomas: experience with explanted livers. Intervirology 2004;47:191–8.
7. Hytiroglou P, Park YN, Krinsky G, Theise ND. Hepatic precancerous lesions and small hepatocellular carcinoma. Gastroenterol Clin N Am 2007;36:867–87.
8. Kudo M. Imaging diagnosis of hepatocellular carcinoma and premalignant/borderline lesions. Semin Liver Dis 1999;19:297–309.
9. Kudo M. Imaging blood flow characteristics of hepatocellular carcinoma. Oncology 2002;62(suppl 1):48–56.
10. Matsui O, Kadoya M, Kameyama T, Yoshikawa J, Takashima T, Nakanuma Y, et al. Benign and malignant nodules in cirrhotic livers: distinction based on blood supply. Radiology 1991;178: 493–7.
11. Choi BI, Takayasu K, Han MC. Small hepatocellular carcinomas and associated nodular lesions of the liver: pathology, pathogenesis, and imaging findings. AJR Am J Roentgenol 1993;160: 1177–87.
12. Takayasu K, Muramatsu Y, Furukawa H, Wakao F, Moriyama N, Takayama T, et al. Early hepatocellular carcinoma: appearance at CT during arterial portography and CT arteriography with pathologic correlation. Radiology 1995;194:101–5.
13. Matsui O, Kadoya M, Kameyama T, Yoshikawa J, Arai K, Gabata T, et al. Adenomatous hyperplastic nodules in the cirrhotic liver: differentiation from hepatocellular carcinoma with MR imaging. Radiology 1989;173:123–6.
14. Muramatsu Y, Nawano S, Takayasu K, Moriyama N, Yamada T, Yamasaki S, et al. Early hepatocellular carcinoma: MR imaging. Radiology 1991;181:209–13.
15. Takayasu K, Shima Y, Muramatsu Y, Goto H, Moriyama N, Yamada T, et al. Angiography of small hepatocellular carcinomas: analysis of 105 resected tumors. AJR Am J Roentgenol 1986;147:525–9.
16. Kudo M, Chung H, Haji S, Osaki Y, Oka H, Seki T, et al. Validation of a new prognostic staging system for hepatocellular carcinoma: the JIS score compared with the CLIP score. Hepatology 2004;40:1396–405.
17. International Working Party. Terminology of nodular hepatocellular lesions. Hepatology 1995;22:983–93.
18. Nakanuma Y, Hirata K, Terasaki S, Ueda K, Matsui O. Analytical histopathological diagnosis of small hepatocellular nodules in chronic liver disease. Histol Histopathol 1998;13:1077–87.
19. Sakamoto M, Hirohashi S, Tsuda H, Shimosato Y, Makuuchi M, Hosoda Y. Multicentric independent development of hepatocellular carcinoma revealed by analysis of hepatitis B virus integration pattern. Am J Surg Pathol 1989;13:1064–7.
20. Nakanuma Y, Terada T, Ueda K, Terasaki S, Nonomura A, Matsui O. Adenomatous hyperplasia of the liver as a precancerous lesion. Liver 1993;13:1–9.
21. Sugihara S, Nakashima O, Kojiro M, Majima Y, Tanaka M, Tanikawa K. The morphologic transition in hepatocellular carcinoma. A comparison of the individual histologic features disclosed by ultrasound-guided fine-needle biopsy with those of autopsy. Cancer (Phila) 1992;70:1488–92.
22. Takayama T, Makuuchi M, Hirohashi S, Sakamoto M, Okazaki N, Takayasu K, et al. Malignant transformation of adenomatous hyperplasia to hepatocellular carcinoma. Lancet 1990;336: 1150–3.
23. Bhattacharya S, Dhillon AP, Rees J, Savage K, Saada J, Burroughs A, et al. Small hepatocellular carcinomas in cirrhotic explant livers: identification by macroscopic examination and lipiodol localization. Hepatology 1997;25:613–8.
24. Mion F, Grozel L, Boillot O, Paliard P, Berger F. Adult cirrhotic liver explants: precancerous lesions and undetected small hepatocellular carcinomas. Gastroenterology 1996;111: 1587–92.
25. Hytiroglou P. Morphological changes of early human hepatocarcinogenesis. Semin Liver Dis 2004;24:65–75.
26. Kojiro M. Pathology of hepatocellular carcinoma. Oxford: Blackwell; 2006.
27. Kutami R, Nakashima Y, Nakashima O, Shiota K, Kojiro M. Pathomorphologic study on the mechanism of fatty change in small hepatocellular carcinoma of humans. J Hepatol 2000;33: 282–9.
28. Fujii K, Takayasu K, Ohkubo T, Muramatsu Y, Mizuguchi Y, Yamasaki S, et al. Imaging of large early and early advanced hepatocellular carcinomas of more than 5 cm in diameter: report of two cases. Hepatogastroenterology 1998;45:1085–92.
29. Kudo M. Atypical large well-differentiated hepatocellular carcinoma with benign nature: a new clinical entity. Intervirology 2004;47:227–37.
30. Kudo M, Tomita S, Kashida H, Mimura J, Okabe Y, Hirasa M, et al. Tumor hemodynamics in hepatic nodules associated with liver cirrhosis: relationship between cancer progression and tumor hemodynamic change. Nippon Shokakibyo Gakkai Zasshi 1991;88:1554–65.
31. Kudo M, Tomita S, Tochio H, Hamada M, Mimura J, Okabe Y, et al. Hemodynamic characteristics of early stage hepatocellular carcinoma. In vivo evaluation with vascular imagings (in Japanese). Acta Hepatol Jpn 1992;33:283–91.
32. Kojiro M, Sugihara S, Nakashima O. Pathomorphologic characteristics of early hepatocellular carcinoma. Gann Monogr Cancer Res 1991;38:S29–38.
33. Okuda K. Early recognition of hepatocellular carcinoma. Hepatology 1986;6:729–38.
34. Okuda K. Hepatocellular carcinoma: recent progress. Hepatology 1992;15:948–63.
35. Murakami T, Hori M, Kim T, Kawata S, Abe H, Nakamura H. Multidetector row CT and MR imaging in diagnosing hepatocellular carcinoma. Intervirology 2004;47:209–26.
36. Takayasu K, Muramatsu Y, Mizuguchi Y, Moriyama N, Ojima H. Imaging of early hepatocellular carcinoma and adenomatous hyperplasia (dysplastic nodules) with dynamic ct and a combination of CT and angiography: experience with resected liver specimens. Intervirology 2004;47:199–208.
37. Matsui O. Imaging of multistep human hepatocarcinogenesis by CT during intra-arterial contrast injection. Intervirology 2004;47:271–6.
38. Yoshimitsu K, Irie H, Aibe H, Tajima T, Nishie A, Asayama Y, et al. Pitfalls in the imaging diagnosis of hepatocellular nodules in the cirrhotic and noncirrhotic liver. Intervirology 2004;47: 238–51.
39. Kudo M. Morphological diagnosis of hepatocellular carcinoma: special emphasis on intranodular hemodynamic imaging. Hepatogastroenterology 1998;45(suppl 3):1226–31.
40. Tochio H, Kudo M. Afferent and efferent vessels of premalignant and overt hepatocellular carcinoma: observation by color Doppler imaging. Intervirology 2004;47:144–53.

41. Kudo M, Tochio H, Zhou P. Differentiation of hepatic tumors by color Doppler imaging: role of the maximum velocity and the pulsatility index of the intratumoral blood flow signal. Intervirology 2004;47:154–61.
42. Fukunaga T, Kudo M, Tochio H, Okabe Y, Orino A. Natural course of small nodular lesions with intranodular preserved portal supply in cirrhotic liver. Oncology 2007;72(suppl 1):24–9.
43. Kudo M. Early detection and curative treatment of early-stage hepatocellular carcinoma. Clin Gastroenterol Hepatol 2005;3: S144–8.
44. Kudo M. New sonographic techniques for the diagnosis and treatment of hepatocellular carcinoma. Hepatol Res 2007;37(suppl 2): S193–9.
45. Kim SR, Hayashi Y, Kudo M, Matsuoka T, Imoto S, Song KB, et al. Hepatocellular carcinoma transforming from dysplastic nodule with background of non-B non-C chronic persistent hepatitis. J Hepatol 2000;33:857–8.
46. Kojiro M. "Nodule-in-nodule" appearance in hepatocellular carcinoma: its significance as a morphologic marker of dedifferentiation. Intervirology 2004;47:179–83.
47. Zheng RQ, Zhou P, Kudo M. Hepatocellular carcinoma with nodule-in-nodule appearance: demonstration by contrast-enhanced coded phase inversion harmonic imaging. Intervirology 2004;47:184–90.
48. Okita K. Management of hepatocellular carcinoma in Japan. J Gastroenterol 2006;41:100–6.
49. Kojiro M. Pathology of hepatocellular carcinoma. In: Okuda K, Tabor E, editors. Liver cancer. New York, Churchill-Livingstone; 1997. p. 165–87.
50. Sakamoto M, Hirohashi S. Natural history and prognosis of adenomatous hyperplasia and early hepatocellular carcinoma: multi-institutional analysis of 53 nodules followed up for more than 6 months and 141 patients with single early hepatocellular carcinoma treated by surgical resection or percutaneous ethanol injection. Jpn J Clin Oncol 1998;28:604–8.
51. Hayashi M, Matsui O, Ueda K, Kawamori Y, Gabata T, Kadoya M. Progression to hypervascular hepatocellular carcinoma: correlation with intranodular blood supply evaluated with CT during intraarterial injection of contrast material. Radiology 2002;225: 143–9.
52. Tajima T, Honda H, Taguchi K, Asayama Y, Kuroiwa T, Yoshimitsu K, et al. Sequential hemodynamic change in hepatocellular carcinoma and dysplastic nodules: CT angiography and pathologic correlation. AJR Am J Roentgenol 2002;178:885–97.
53. Kudo M. Contrast harmonic imaging in the diagnosis and treatment of hepatic tumors. Berlin: Springer; 2003.
54. Wen YL, Kudo M, Zheng RQ, Ding H, Zhou P, Minami Y, et al. Characterization of hepatic tumors: value of contrast-enhanced coded phase-inversion harmonic angio. AJR Am J Roentgenol 2004;182:1019–26.
55. Imai Y, Murakami T, Yoshida S, Nishikawa M, Ohsawa M, Tokunaga K, et al. Superparamagnetic iron oxide-enhanced magnetic resonance images of hepatocellular carcinoma: correlation with histological grading. Hepatology 2000;32:205–12.
56. Asahina Y, Izumi N, Uchihara M, Noguchi O, Ueda K, Inoue K, et al. Assessment of Kupffer cells by ferumoxides-enhanced MR imaging is beneficial for diagnosis of hepatocellular carcinoma: comparison of pathological diagnosis and perfusion patterns assessed by CT hepatic arteriography and CT arterioportography. Hepatol Res 2003;27:196–204.
57. Kudo M, Okanoue T, Japan Society of Hepatology. Management of hepatocellular carcinoma in Japan: consensus-based clinical practice manual proposed by the Japan Society of Hepatology. Oncology 2007;72(suppl 1):2–15.

Case Report

Digestion

Digestion 2009;79:36–39
DOI: 10.1159/000203639

Published online: February 25, 2009

Pegylated Interferon plus Ribavirin Combination Therapy for Chronic Hepatitis C with High Viral Load of Serum Hepatitis C Virus RNA, Genotype 1b, Discontinued on Attaining Sustained Virological Response at Week 16 after Onset of Acute Pancreatitis

Soo Ryang Kim[c] Susumu Imoto[c] Keiji Mita[c] Miyuki Taniguchi[c]
Noriko Sasase[c] Akira Muramatsu[a] Masatoshi Kudo[b] Satoshi Kitai[b]
Ahmed El-Shamy[d] Hak Hotta[d] Yoshitake Hayashi[e]

[a]Division of Liver Diseases, Meimai Central Hospital, Akashi, [b]Department of Gastroenterology and Hepatology, Kinki University School of Medicine, Osaka-Sayama, [c]Department of Gastroenterology, Kobe Asahi Hospital, [d]Division of Microbiology, and [e]Division of Molecular Medicine and Medical Genetics, International Center for Medical Research and Treatment, Kobe University Graduate School of Medicine, Kobe, Japan

Key Words
Acute pancreatitis · Chronic hepatitis C · Early viral dynamics, genotype 1b · Sustained virological response

Abstract
Recent clinical trials have shown that pegylated interferon-α (PEG-IFN-α) in combination with ribavirin (RBV) improves the rate of sustained virological response (SVR), with over 50% of patients demonstrating a positive response to treatment. However, no SVR has been reported when PEG-IFN/RBV combination therapy is discontinued by week 16, especially in cases of chronic hepatitis with a high viral load of serum hepatitis C virus (HCV) RNA, genotype 1b. Here, we describe SVR in a 67-year-old woman whose PEG-IFN/RBV combination therapy for chronic hepatitis C with a high viral load of serum HCV RNA, genotype 1b, was discontinued after 16 weeks because of the onset of PEG-IFN plus RBV-induced acute pancreatitis. Among viral factors, substitution of amino acid 70 (Arg) and 91 (Leu) in the core region and HCV RNA negativity were observed after 8 weeks. Host factors including low body weight, no alcohol consumption, no coinfection with hepatitis B virus, slight fibrosis, and viral factors including early viral clearance, double wild type in the core region, may have contributed to the SVR irrespective of the discontinuation of the combination therapy at week 16. Moreover, PEG-IFN plus RBV-induced acute pancreatitis might have been related to the SVR.

Introduction

In Japan, about 70% of chronic hepatitis C (CHC) patients are infected with genotype 1b, the rest with genotype 2a/2b [1]. Of the former, almost 70% demonstrate a high viral load, a crucial risk factor for poor response to antiviral treatment, as are the host-related factors of age, obesity, female gender and hepatic fibrosis [2, 3].

The rate of sustained virological response (SVR) can be increased to approximately 40% through 48 weeks of interferon (IFN)-α2b and ribavirin (RBV) combination

KARGER
Fax +41 61 306 12 34
E-Mail karger@karger.ch
www.karger.com

0012–2823/09/0791–0036$26.00/0

Accessible online at:
www.karger.com/dig

Soo Ryang Kim, MD
Department of Gastroenterology, Kobe Asahi Hospital
3-5-25 Bououji-cho, Nagata-ku, Kobe 653-0801 (Japan)
Tel. +81 78 612 5151, Fax +81 78 612 5152
E-Mail asahi-hp@arion.ocn.ne.jp

therapy for chronic hepatitis with a high viral load of serum hepatitis C virus (HCV) RNA, genotype 1b [4–6]. Pegylated (PEG)-IFN-α plus RBV therapy improves the SVR rate even further, with over 50% of patients responding positively to treatment [6]. Attaining the SVR irrespective of discontinuing combination therapy by week 16 has not been reported, even in cases of rapid virological response by CHC with a high viral load of serum HCV RNA, genotype 1b [7, 8].

Acute pancreatitis is an uncommon side effect of IFN-α and RBV combination therapy, and only few cases have been reported in the English literature [9]. It has also been diagnosed in 7 of 1,706 HCV-infected patients (0.4%; 95% CI 0.2–0.8) thus treated [10]. We present the case of a 67-year-old woman with chronic hepatitis and a high viral load of serum HCV RNA, genotype 1b, attaining SVR and discontinuing the therapy after 16 weeks because of the onset of acute pancreatitis after 14 weeks of therapy.

Case Report

A 67-year-old woman with CHC was admitted to Kobe Asahi Hospital in September 2007 for treatment of abdominal pain. In June 2007, she had been started on a weekly subcutaneous injection of 60 μg of PEG-IFN-α2b and a daily oral dose of 600 mg RBV at 44 kg of body weight. Reverse transcription polymerase chain reaction (PCR) revealed 2,300 and 1,900 kIU/ml of HCV RNA in May 2007 and June 2007, respectively. Hepatitis B surface antigen and hepatitis B virus DNA were negative, HCV core antigen by a new immunoradiometric (IRM) assay was 5,550 fmol/l, and the genotype was 1b. Laboratory tests revealed the following: total protein 6.2 g/dl (normal, 6.5–8.3), albumin 3.8 g/dl (3.8–5.3), aspartate aminotransferase 40 IU/l (0–38), alanine aminotransferase 29 IU/l (0–19), platelets 13.9 × 10^4/μl (14–34); liver biopsy revealed stage 1 fibrosis. Immunological examinations revealed the following: immunoglobulin G (IgG) 1,460 mg/dl (normal, 870–1,700), IgM 168 mg/dl (33–190), IgA 76 mg/dl (110–410), B cells 4% (4–13), T cells 90% (66–89), CD4/CD8 ratio 1.17% (0.40–2.30) and natural killer cell activity 50% (18–40).

Viral factors considered to be related to SVR [11–14] were as follows: 4 IFN/RBV resistance-determining region mutants (SVR is related to more than 6), 0 IFN sensitivity-determining region mutants (SVR is related to more than 4), and the core protein was the double wild type (Arg 70/Leu 91; SVR is related to the double wild type). Regarding early viral dynamics, HCV core antigen was 1,670 fmol/l at 24 h, 118 fmol/l at 1 week and <20 fmol/l at 2 weeks after treatment; it was <20 fmol/l, irrespective of HCV RNA positivity, 4 weeks after treatment. After 8 weeks, HCV RNA by the Amplicore PCR method was undetectable (<50 copies/ml) and liver functions were normal.

The patient tolerated therapy well until week 14, when she was admitted to our hospital with severe epigastric pain radiating to her back, nausea and vomiting. Laboratory tests revealed the following: amylase 178 IU/l (normal, 38–136), lipase 521 IU/l (23–300), aspartate aminotransferase 29 IU/l, alanine aminotransferase 10 IU/l, alkaline phosphokinase 226 IU/l (110–354), total bilirubin 0.5 mg/dl (0.2–1.2), white blood cell count 50 × 10^2/μl (40–90), calcium 9.4 mg/dl (8.7–10.1), total cholesterol 140 mg/dl (150–219), triglycerides 153 mg/dl (50–149), IgG4 20.1 mg/dl (48–105); all values, except for triglycerides and IgG4, were within normal limits. Tumor necrosis factor-α (TNF-α) and IL-6 were 8.8 pg/ml (<5.0) and 3.4 pg/ml (<4.0), respectively. The patient had no history of pancreatitis, denied alcohol use and was not taking any medications. Imaging studies such as ultrasound, computed tomography and magnetic resonance imaging revealed no swelling of the pancreas or dilation of the pancreatic duct. The gallbladder appeared normal and no biliary microgallstones were noted.

PEG-IFN-α2b and RBV were discontinued 16 weeks after the start of therapy, and the patient was treated with ulinastatin 150,000 units/day for 4 weeks and camostat mesilate 600 mg/day (oral dose) for 2 weeks under the diagnosis of acute pancreatitis. The pancreatitis was resolved and the patient was discharged in December 2007.

PEG-IFN-α2b and RBV therapy was discontinued and pancreatitis did not recur during 12 months of follow-up. Since January 2008, HCV has been undetectable (<15 copies/ml) by the TaqMan PCR method, and liver functions continued normal. The patient was evaluated as having attained SVR because HCV RNA disappeared 52 weeks after the discontinuation of therapy (fig. 1).

Discussion

Acute pancreatitis is a rare complication of PEG-IFN/RBV therapy. In our case, drug-induced acute pancreatitis was diagnosed on the basis of the presence of epigastric pain, elevated amylase and lipase levels, and the absence of other identifiable causes of pancreatitis. The patient showed no evidence of gallstones, alcohol consumption, or other potential causes of pancreatitis, such as autoimmune pancreatitis. These findings met the criteria for probable drug-induced pancreatitis [15, 16]. The onset of pancreatitis during PEG-IFN-α2b and RBV therapy and resolution of the symptoms after the discontinuation of treatment confirmed the diagnosis. Moreover, the absence of recurrent pancreatitis after the discontinuation of therapy also suggested that the medications were the most likely cause of acute pancreatitis.

IFN and RBV combination therapy is a potential cause of drug-induced pancreatitis in patients with chronic HCV. There are several potential mechanisms whereby IFN-α can cause pancreatitis. Treatment with IFN-α can result in severe hypertriglyceridemia [17–19], a well-described cause of acute pancreatitis [20]. However, in our case, severe hypertriglyceridemia was not observed. Alternatively, IFN-α may cause acute pancreatitis by stimu-

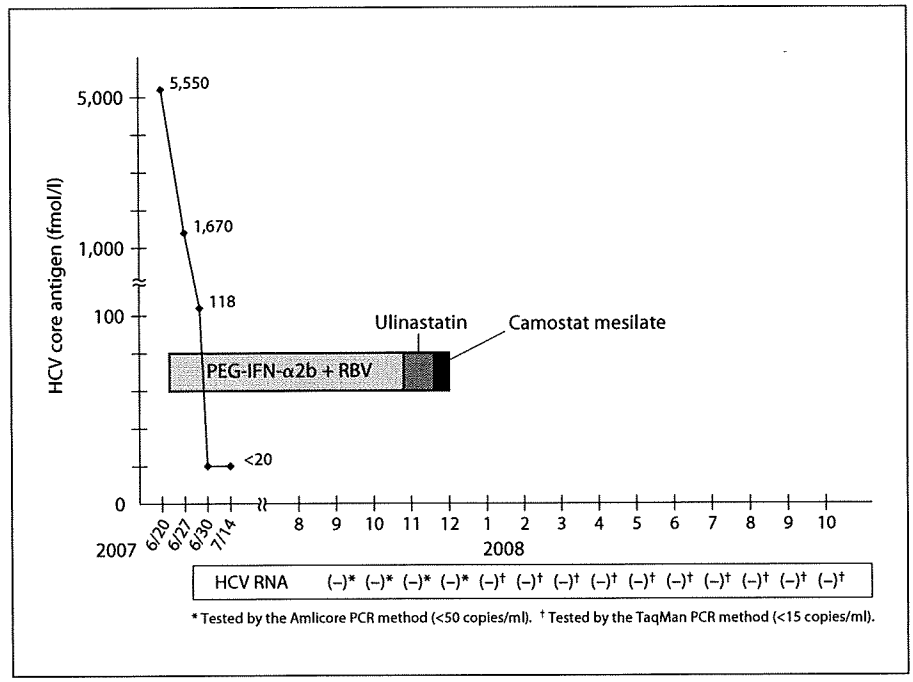

Fig. 1. Clinical course.

lating the immune system, leading to autoimmune destruction of the pancreas. In fact, IFN-α is known to precipitate or exacerbate other autoimmune disorders, such as thyroid disease, diabetes and others [21]. Based on the published literature, IFN-α is more likely to cause acute pancreatitis than RBV, although RBV is known to have immunomodulatory effects [22]; also, RBV, alone or synergistically with IFN-α, may stimulate the immune system to cause pancreatitis through an autoimmune mechanism. TNF-α is reported to induce acute pancreatitis [23]. In our case, high TNF-α may be markers of immune system stimulation due to PEG-IFN plus RBV or due to acute pancreatitis itself [24].

Predictors of the outcome of IFN-based therapy can be classified into pretreatment and on-treatment factors. The former comprise host factors such as age, sex, obesity, alcohol consumption, fibrosis, immune responses, as well as coinfection with other viruses, and the latter comprise viral factors that include mainly viral genotypes and viral load. In our case, viral genotype (genotype 1b) and high viral load (2,300 kIU/ml), old age (67 years) and sex (female) were poor response factors to the therapy. Low body weight, no alcohol consumption, no coinfection with other viruses, such as hepatitis B virus, and slight fibrosis (F1) were favorable factors for the SVR. Immunological examinations including the percentage of B cells, T cells and the CD4/CD8 ratio were within almost normal limits, except for high natural killer cell activity; consequently, immunologic activity does not explain the SVR in our case.

On-treatment factors are mainly related to viral kinetics within the first few weeks of treatment [25]. A new IRM assay of HCV core antigen is very useful in predicting virological response during PEG-IFN/RBV combination therapy for chronic hepatitis with a high viral load of serum HCV RNA, genotype 1b [26]. Our patient demonstrated a rapid virological decrease in HCV core antigen during 4 weeks after the start of therapy, as revealed by the new IRM assay.

Because the HCV genotype is one of the major factors affecting the response to IFN-based therapy, resistance to IFN is, at least partly, genetically encoded by HCV itself [27]. In this context, nonstructural protein 5A (NS5A), one of the HCV nonstructural proteins, has been widely discussed for its correlation with IFN responsiveness. Sequence variations within a region in NS5A, called 'IFN sensitivity-determining region', have been proposed as correlated with IFN responsiveness [12, 13]. A high degree of sequence variations in the V3 [amino acids (aa) 2356–2379] and the pre-V3 regions (aa 2334–2355) of NS5A, collectively referred to as the 'IFN/RBV resistance-determining region' (aa 2334–2379), is closely correlated with SVR in HCV-1b-infected patients treated with PEG-IFN and RBV [11]. Substitutions of aa

70 (Arg) and 91 (Leu) in the core region (double wild type) are correlated with IFN responsiveness [14]. In our case, only 1 virological factor, the double wild type in the core region, among these 3 virological factors considered to be correlated with SVR, was compatible with SVR.

In conclusion, host factors and viral factors may have contributed to SVR in our case, irrespective of the discontinuation of therapy after 16 weeks. Moreover, acute pancreatitis with high TNF-α might have been related to the SVR. Further study is needed to elucidate the host and viral factors correlated with SVR.

References

1 Yoshizawa H: Trends of hepatitis virus carriers. Hepatol Res 2002;24:S28–S39.
2 Hiramatsu N, Oze T, Tsuda N, Kurashige N, Koga K, Toyama T, Yasumru M, Kanto T, Takehara T, Kasahara A, Kato M, Yoshihara H, Katayama K, Hijioka T, Hagiwara H, Kubota S, Oshita M, Haruna Y, Mita E, Suzuki K, Ishibashi K, Hayashi N: Should aged patients with chronic hepatitis C be treated with interferon and ribavirin combination therapy? Hepatol Res 2006;35:185–189.
3 Charlton MR, Pockros PJ, Harrison SA: Impact of obesity on treatment of chronic hepatitis C. Hepatology 2006;43:1177–1186.
4 McHutchison JG, Gordon SC, Schiff ER, Shiffman ML, Lee WM, Rustgi VK, Goodman ZD, Ling MH, Cort S, Albrecht JK: Interferon alfa-2b alone or in combination with ribavirin as initial treatment for chronic hepatitis C. Hepatitis Interventional Therapy Group. N Engl J Med 1998;339:1485–1492.
5 Poynard T, Marcellin P, Lee SS, Niederau C, Minuk GS, Ideo G, Bain V, Heathcote J, Zeuzem S, Trepo C, Albrecht J: Randomized trial of interferon alpha 2b plus ribavirin for 48 weeks or for 24 weeks versus interferon alpha 2b plus placebo for 48 weeks for treatment of chronic infection with hepatitis C virus. International Hepatitis Interventional Therapy Group. Lancet 1998;352:1426–1432.
6 Manns MP, McHutchison JG, Gordon SC, Rustgi VK, Shiffman M, Reindollar R, Goodman ZD, Koury K, Ling M, Albrecht JK: Peginterferon alfa-2b plus ribavirin compared with interferon alfa-2b plus ribavirin for initial treatment of chronic hepatitis C: a randomized trial. Lancet 2001;358:958–965.
7 Fried MW, Shiffman ML, Reddy KR, Smith C, Marinos G, Gonçales FL Jr, Häussinger D, Diago M, Carosi G, Dhumeaux D, Craxi A, Lin A, Hoffman J, Yu J: Peginterferon alfa-2a plus ribavirin for chronic hepatitis C virus infection. N Engl J Med 2002;347:975–982.
8 Jensen DM, Morgan TR, Marcellin P, Pockros PJ, Reddy KR, Hadziyannis SJ, Ferenci P, Ackrill AM, Willems B: Early identification of HCV genotype 1 patients responding to 24 weeks peginterferon alpha-2a (40 kd)/ribavirin therapy. Hepatology 2006;43:954–960.
9 Eland IA, Rasch MC, Sturkenboom MJ, Bekkering FC, Brouwer JT, Delwaide J, Belaiche J, Houbiers G, Stricker BH: Acute pancreatitis attributed to the use of interferon alfa-2b. Gastroenterology 2000;119:230–233.
10 Chaudhari S, Park J, Anand BS, Pimstone NR, Dieterich DT, Batash S, Bini E: Acute pancreatitis associated with interferon and ribavirin therapy in patients with chronic hepatitis C. Dig Dis Sci 2004;49:1000–1006.
11 El-Shamy A, Nagano-Fujii M, Sasase N, Imoto S, Kim SR, Hotta H: Sequence variation in hepatitis C virus nonstructural protein 5A predicts clinical outcome of pegylated interferon/ribavirin combination therapy. Hepatology 2008;48:38–47.
12 Enomoto N, Sakuma I, Asahina Y, Kurosaki M, Murakami T, Yamamoto C, Izumi N, Marumo M, Sato C: Comparison of full-length sequences of interferon-sensitive and resistant hepatitis C virus 1b: sensitivity to interferon is conferred by amino acid substitutions in the NS5A region. J Clin Invest 1995;96:224–230.
13 Enomoto N, Sakuma I, Asahina Y, Kurosaki M, Murakami T, Yamamoto C, Ogura Y, Izumi N, Marumo F, Sato C: Mutations in the nonstructural protein 5A gene and response to interferon in patients with chronic hepatitis C virus 1b infection. N Engl J Med 1996; 334:77–81.
14 Akuta N, Suzuki F, Kawamurua Y, Yatsuji H, Sezaki H, Suzuki Y, Hosaka T, Kobayashi M, Kobayashi M, Arase Y, Ikeda K, Kumada H: Predicative factors of early and sustained responses to peginterferon plus ribavirin combination therapy in Japanese patients infected with hepatitis C virus genotype 1b: amino acid substitutions in the core region and low-density lipoprotein cholesterol levels. J Hepatol 2007;46:403–410.
15 Mallory A, Kern F Jr: Drug-induced pancreatitis: a critical review. Gastroenterology 1980;78:813–820.
16 McArthur KE: Review article: drug-induced pancreatitis. Aliment Pharmacol Ther 1996; 10:23–38.
17 Fernández-Miranda C, Castellano G, Guijarro C, Fernández I, Schöebel N, Larumbe S, Gómez-Izquierdo T, del Palacio A: Lipoprotein changes in patients with chronic hepatitis C treated with interferon-alpha. Am J Gastroenterol 1998;93:1901–1904.
18 Naeem M, Bacon BR, Mistry B, Britton RS, Di Bisceglie AM: Changes in serum lipoprotein profile during interferon therapy in chronic hepatitis C. Am J Gastroenterol 2001;96:2468–2472.
19 Shinohara E, Yamashita S, Kihara S, Hirano K, Ishigami M, Arai T, Nozaki S, Kameda-Takemura K, Kawata S, Matsuzawa Y: Interferon alpha induces disorder of lipid metabolism by lowering postheparin lipases and cholesteryl ester transfer protein activities in patients with chronic hepatitis C. Hepatology 1997;25:1502–1506.
20 Steinberg W, Tenner S: Acute pancreatitis. N Engl J Med 1994;330:1198–1210.
21 Russo MW, Fried MW: Side effects of therapy for chronic hepatitis C. Gastroenterology 2003;124:1711–1719.
22 Snell NJ: Ribavirin – current status of a broad spectrum antiviral agent. Expert Opin Pharmacother 2001;2:1317–1324.
23 Malleo G, Mazzon E, Siriwardena AK, Cuzzocrea S: Role of tumor necrosis factor-alpha in acute pancreatitis: from biological basis to clinical evidence. Shock 2007;28:130–140.
24 Zhang XP, Lin Q, Zhou YF: Progress of study on the relationship between mediators of inflammation and apoptosis in acute pancreatitis. Dig Dis Sci 2007;52:1199–1205.
25 Ferenci P: Predictors of response to therapy for chronic hepatitis C. Semin Liver Dis 2004;24:S25–S31.
26 Sasase N, Kim SR, Kim KI, Taniguchi M, Imoto S, Mita K, Hotta H, Shouji I, El-Shamy A, Kawada N, Kudo M, Hayashi Y: Usefulness of a new immunoradiometric assay of HCV core antigen to predict virological response during PEG-IFN/RBV combination therapy for chronic hepatitis with high viral load of serum HCV RNA genotype 1b. Intervirology 2008;51:S70–S75.
27 Welker MW, Hofmann WP, Welsch C, von Wagner M, Herrmann E, Lengauer T, Zeuzem S, Sarrazin C: Correlation of amino acid variations within nonstructural 4B protein with initial viral kinetics during interferon-alpha-based therapy in HCV-1b-infected patients. J Viral Hepatol 2007;14:338–349.

Hepatol Int (2009) 3:411–415
DOI 10.1007/s12072-009-9128-z

CASE REPORT

Well-differentiated hepatocellular carcinoma smaller than 15 mm in diameter totally eradicated with percutaneous ethanol injection instead of radiofrequency ablation

Soo Ryang Kim · Susumu Imoto · Taisuke Nakajima · Kenji Ando · Keiji Mita · Miyuki Taniguchi · Noriko Sasase · Toshiyuki Matsuoka · Masatoshi Kudo · Yoshitake Hayashi

Received: 14 December 2008 / Accepted: 5 March 2009 / Published online: 21 March 2009

Abstract We describe three cases of well-differentiated hepatocellular carcinoma (HCC) smaller than 15 mm in diameter completely eradicated with percutaneous ethanol injection (PEI) instead of using radiofrequency ablation (RFA). Ultrasound (US) examination revealed one nodule each in segment 2 (hypoechoic, near bile ducts, 10 mm), in segment 5 (hyperechoic, near the gall bladder, 15 mm), and in segment 7 (hypoechoic, near the diaphragm, 15 mm). Although imaging studies revealed isovascular (case 1) and hypervascular (cases 2 and 3) nodules, histological analysis of US-guided biopsy tissue revealed well-differentiated HCC. In consideration of the location of the nodules, PEI, instead of RFA, was administered and the nodules were rendered necrotic. Although RFA is superior to PEI in the treatment of small HCCs from the viewpoint of treatment response and long survival, PEI is strongly recommended for HCCs located near bile ducts, the gall bladder, and the diaphragm, especially when the nodules are smaller than 15 mm in diameter.

Keywords Percutaneous ethanol injection · Bile ducts · Gall bladder · Diaphragm · HCC smaller than 15 mm in diameter

S. R. Kim (✉) · S. Imoto · T. Nakajima · K. Ando · K. Mita · M. Taniguchi · N. Sasase
Department of Gastroenterology, Kobe Asahi Hospital, 3-5-25 Bououji-cho, Nagata-ku, Kobe 653-0801, Japan
e-mail: asahi-hp@arion.ocn.ne.jp

T. Matsuoka
Department of Radiology, Osaka City University Medical School, Osaka, Japan

M. Kudo
Department of Gastroenterology and Hepatology, Kinki University School of Medicine, Osaka-Sayama, Japan

Y. Hayashi
Division of Molecular Medicine & Medical Genetics, International Center for Medical Research and Treatment (ICMRT), Kobe University Graduate School of Medicine, Kobe, Japan

Introduction

Hepatocellular carcinoma (HCC) is one of the major malignancies worldwide [1–4]. With recent advances in diagnostic imaging, particularly in ultrasound (US), an increasing number of small or early-stage HCCs have been detected. In patients with early-stage HCC, percutaneous ethanol injection (PEI) is a second choice when surgical techniques have been precluded. Over the past few years, however, several methods of thermal tumor eradication through localized heating or freezing, including radiofrequency ablation (RFA), laser ablation, microwave ablation, and cryoablation, have been developed and clinically tested. Among these, RFA has recently emerged as a real competitor to PEI.

Indeed, RFA is superior to PEI in the treatment of small HCCs from the viewpoint of treatment response and long-term survival [5–7]. It is difficult, however, to apply to tumors located near bile ducts, the gall bladder, and the diaphragm. In contrast, PEI is feasible, efficacious, and very safe.

We describe three cases of well-differentiated HCCs smaller than 15 mm in diameter located near bile ducts, the gall bladder, and the diaphragm, completely eradicated with PEI instead of using RFA.

Case reports

Case 1

A 73-year-old woman with hepatitis C virus (HCV)-related cirrhosis (Child-Pugh A class) was admitted to Kobe Asahi Hospital for further examination of a 10-mm hyperechoic nodule in segment 2 (S2) near the bile ducts. The levels of tumor markers in March 2007 were as follows: α-fetoprotein (AFP) 26 ng/ml (normal: ≤10.0), lens culinaris agglutinin A-reactive fraction of AFP (AFP L3) 4.0% (<10.0), and protein induced by vitamin K absence (PIVKA-II) 14 mAU/ml (≤40). Contrast-enhanced US revealed isovascularity in both the early- and postvascular phases. Contrast-enhanced computed tomography (CT) revealed an isovascular nodule in the early phase and washout in the late phase (Fig. 1a). Histologically, the nodule was a well-differentiated HCC characterized by more than twofold the cellularity of the nontumorous area and mild cell atypia with a thin trabecular pattern (Fig. 1b). PEI was administered (three sessions; twice a week) by 1 to 2 injections of 95% sterile ethyl alcohol (total 10.4 ml) delivered to the nodule with a multiple side-hole 21-gauge needle (Et-hanoject, TSK, Tokyo, Japan). After that, contrast-enhanced CT revealed a low-density area (LDA) (Fig. 1c), and, histologically, US-guided biopsy revealed complete necrosis of the nodule. The levels of tumor markers revealed the following values: AFP 14.4 ng/ml, AFP L3 3.7%, and PIVKA-II 14 mAU/ml. No local recurrence, metachronous tumors, or distant metastases of the original tumor have been observed for 22 months since PEI.

Case 2

A 55-year-old man with hepatitis B virus-related chronic hepatitis was admitted to Kobe Asahi Hospital for further examination of a 15-mm hyperechoic nodule in segment 5 (S5) near the gall bladder. The levels of tumor markers in May 2007 were as follows: AFP 4.9 ng/ml and PIVKA-II 19 mAU/ml. Contrast-enhanced US revealed hypervascularity in the early phase and defect in the Kupffer phase. Contrast-enhanced CT revealed a ring-shaped enhancement in the early phase (Fig. 2a) and washout in the late phase. Histologically, the nodule was a well-differentiated HCC characterized by more than twofold the cellularity of the nontumorous area and mild cell atypia with a thin trabecular pattern (Fig. 2b). PEI was administered (three sessions; twice a week) by 1 to 2 injections of 95% sterile ethyl alcohol (total 15.5 ml) delivered to the nodule with a multiple side-hole 21-gauge needle (Et-hanoject, TSK, Tokyo, Japan). After that, contrast-enhanced CT revealed an LDA or no enhancement (Fig. 2c), and, histologically, US-guided biopsy revealed complete necrosis of the nodule. The levels of tumor markers revealed the following values: AFP 2.9 ng/ml and PIVKA-II 19 mAU/ml. No local recurrence, metachronous tumors, or distant metastases of the original tumor have been observed for 18 months since PEI.

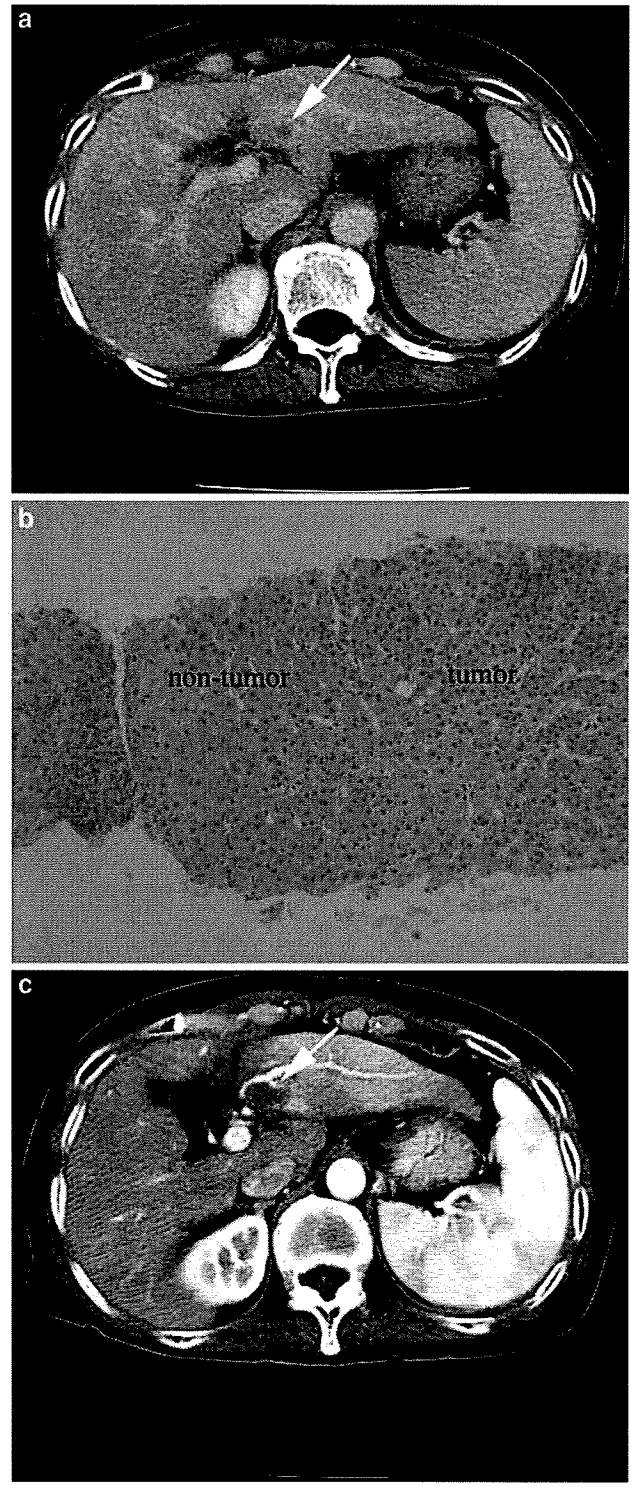

Fig. 1 Before PEI: (**a**) contrast-enhanced CT revealed washout in the late phase (*arrow*); (**b**) well-differentiated HCC was observed. After PEI: (**c**) contrast-enhanced CT revealed an LDA (*arrow*)

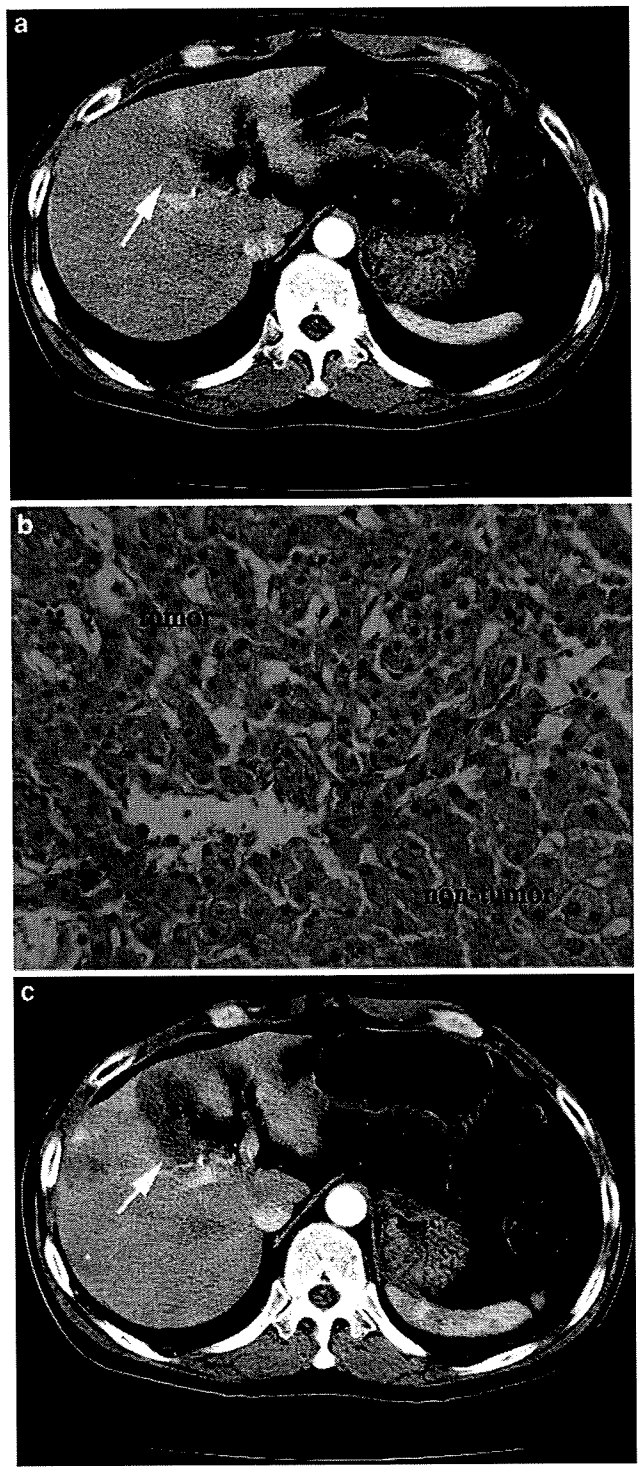

Fig. 2 Before PEI: (**a**) contrast-enhanced CT revealed a ring-shaped enhancement in the early phase (*arrow*); (**b**) well-differentiated HCC was observed. After PEI: (**c**) contrast-enhanced CT revealed an LDA or no enhancement (*arrow*)

Case 3

A 71-year-old man with HCV-related cirrhosis (Child-Pugh A class) was admitted to Kobe Asahi Hospital for further examination of a 15-mm hypoechoic nodule in segment 7 (S7) near the diaphragm. The levels of tumor markers in October 2007 were as follows: AFP 5.3 ng/ml and PIVKA-II 39 mAU/ml. Contrast-enhanced US revealed isovascularity in the early phase and defect in the Kupffer phase. Contrast-enhanced CT and magnetic imaging resonance revealed isovascularity in both the early and late phases. CT during arteriography disclosed slight hypervascularity (Fig. 3a) and CT during arterial portography revealed perfusion defect. Histologically, the nodule was a well-differentiated HCC characterized by more than twofold the cellularity of the nontumorous area and mild cell atypia with a thin trabecular pattern (Fig. 3b). PEI was administered (six sessions; twice a week) by 1 to 2 injections of 95% sterile ethyl alcohol (total 48.0 ml) delivered to the nodule with a multiple side-hole 21-gauge needle (Et-hanoject, TSK, Tokyo, Japan). After that, contrast-enhanced CT revealed an LDA (Fig. 3c), and, histologically, US-guided biopsy revealed complete necrosis of the nodule. The levels of tumor markers revealed the following values: AFP 3.6 ng/ml and PIVKA-II 24 mAU/ml. No local recurrence, metachronous tumors, or distant metastases of the original tumor have been observed for 14 months since PEI.

Discussion

PEI has been the standard therapy since the late 20th century; however, a drastic shift from PEI to RFA has recently been introduced into clinical practice because effective ablation seems more readily attainable with RFA than with PEI or microwave coagulation. Most trials comparing RFA and PEI for the treatment of small HCCs have demonstrated not only local efficacy but also survival in favor of RFA.

In a comparison of PEI and RFA on 86 patients with 112 HCCs [5], complete response was reached in 90.3% by RFA and 80% by PEI, with an average of 1.2 and 4.8 sessions, respectively. In a study of 232 patients (118 treated with RFA and 114 treated with PEI), the 4-year survival rate was 74% (95% confidence interval [CI] 65–84) for RFA and 57% (95% CI 45–71) for PEI, with a 46% smaller risk of death (adjusted relative risk, 0.54 [95% CI 0.33–0.89], $P = 0.02$), a 43% smaller risk of overall recurrence (adjusted relative risk, 0.57 [95% CI 0.41–0.80], $P = 0.0009$), and an 88% smaller risk of local tumor progression (relative risk, 0.12 [95% CI 0.03–0.55], $P = 0.006$) with RFA than with PEI [6]. Similarly, longer survival has also been suggested by the analysis of a subgroup trial in Taiwan [7], and Cho et al. [8] have reported that RFA demonstrates significantly improved 3-year survival status by the meta-analysis of four randomized

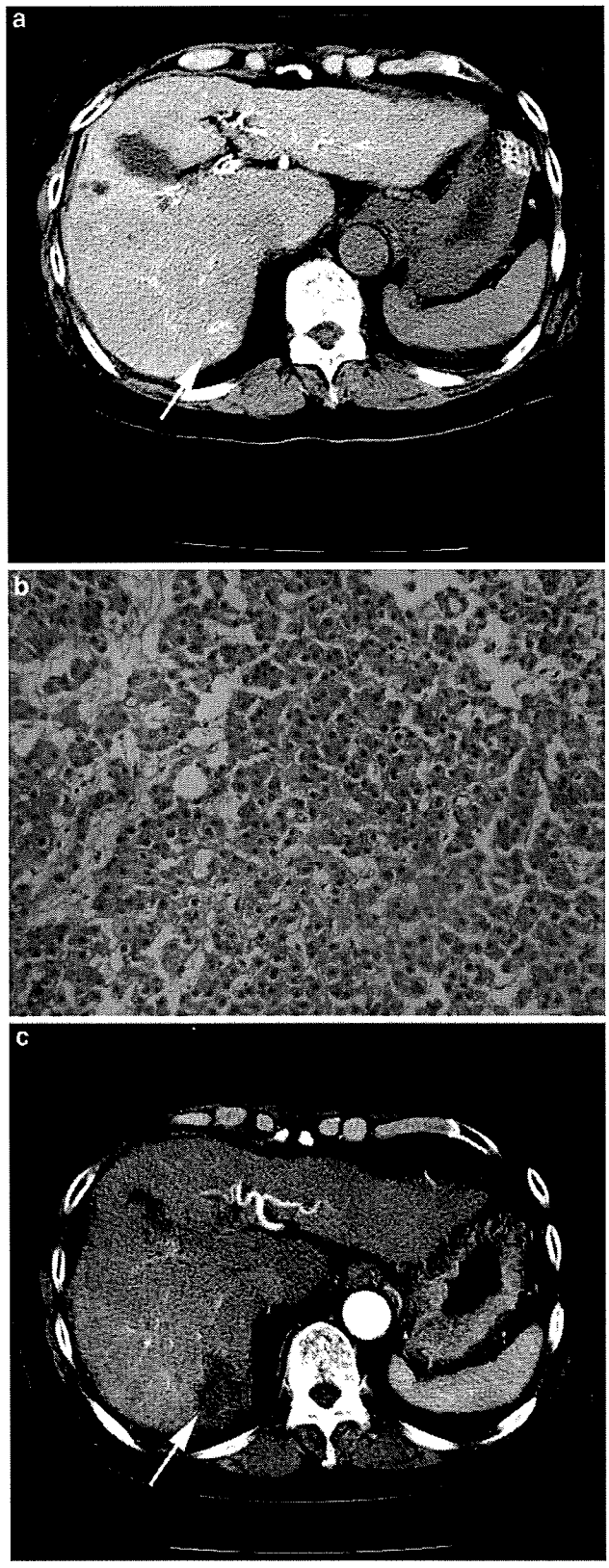

Fig. 3 Before PEI: (**a**) CTA revealed slight hypervascularity (*arrow*); (**b**) well-differentiated HCC was observed. After PEI: (**c**) contrast-enhanced CT revealed an LDA (*arrow*)

controlled trails. Moreover, RFA requires shorter hospitalization than PEI, which improves the quality of life.

Between January 1999 and May 2002, a total of 3,891 RFAs carried out percutaneously on 2,542 patients, laparoscopically on 23 patients, and surgically on 49 patients (total 2,614 patients) has demonstrated severe complications such as hemothorax, intraperitoneal bleeding, liver abscess, and liver infarction compared with none after PEI in 207 of the 2,614 patients (7.9%) and 9 (0.3%) deaths within 3 months after RFA: 3 from liver failure, 3 from rapid progression and sarcomatous changes, and 1 each from biliary injury, gastrointestinal bleeding, and acute myocardial infarction [9].

Notably, when RFA is done on HCCs near bile ducts, the gall bladder, and the diaphragm, the incidence of complications is more frequent. Twenty-five cases of biliary injury and biloma have been described among 2,614 cases [9], and three cases of late-onset diaphragmatic hernia after RFA of HCC have resulted in death [10, 11]. In our cases, the HCCs were located near bile ducts (case 1), the gall bladder (case 2), and the diaphragm (case 3).

According to extensive clinical and pathological studies on early-stage small HCCs in the past two decades, it has become evident that the majority of small HCCs up to around 20 mm in diameter are composed of well-differentiated cancerous tissues that lack the remarkable cellular and structural atypia seen in classical HCCs [4, 12–16]. Pathological studies on HCCs have shown, however, that tumor size is crucial in microscopic portal invasion and local metastasis. Strictly speaking, the difference in the size of tumors between 15 and 16–20 mm in diameter is significant.

The frequency of portal invasion is significantly lower in 11–15 mm (25%) than in 16–20 mm (40%) HCCs ($P < 0.01$) [17, 18]. Extranodular growth has been found in 5.3% of distinctly nodular tumors <15 mm and in 16.7% of those 16–20 mm in diameter [19]. Accordingly, local ablation therapy for small, distinctly nodular HCCs (16–20 mm) necessitates the ablation of at least a 10-mm wide margin of surrounding tissue to prevent local recurrence from extranodular tumor growth and/or from micrometastasis in the vicinity of the tumor [5]. In general, RFA is superior to PEI for tumor control. PEI, however, can almost totally ablate HCCs 11–15 mm in diameter [20], although the demonstration of complete necrosis by percutaneous core biopsy would not confirm complete tumor necrosis. In conclusion, from the viewpoint of safety, feasibility, and tumor control, we administered PEI, instead of RFA, for well-differentiated HCCs smaller than 15 mm in diameter, located near the bile ducts, the gall bladders, and the diaphragm. Further follow-up is needed to clarify the prognosis of these three cases.

References

1. Edmondson HA, Steiner PE. Primary carcinoma of the liver: a study of 100 cases among 48,900 necropsies. Cancer 1954; 7:462–503
2. Okuda K, Peteres RL, Simson IW. Gross anatomic features of hepatocellular carcinoma from three disparate geographic areas. Proposal of new classification. Cancer 1984;54:2165–2173
3. Trevisani F, Caraceni P, Bernardi M, D'Intino PE, Arienti V, Amorati P, et al. Gross pathologic types of hepatocellular carcinoma in Italian patients. Relationship with demographic, environmental, and clinical factors. Cancer 1993;72:1557–1563
4. Okuda K. Early recognition of hepatocellular carcinoma. Hepatology 1986;6:729–738
5. Livraghi T, Goldberg SN, Lazzaroni S, Meloni F, Solbiati L, Gazelle GS. Small hepatocellular carcinoma: treatment with radio-frequency ablation versus ethanol injection. Radiology 1999;210:655–661
6. Shiina S, Teratani T, Obi S, Sato S, Tateishi R, Fujishima T, et al. A randomized controlled trial of radiofrequency ablation with ethanol injection for small hepatocellular carcinoma. Gastroenterology 2005;129:122–130
7. Lin SM, Lin CJ, Lin CC, Hsu CW, Chen YC. Radiofrequency ablation improves prognosis compared with ethanol injection for hepatocellular carcinoma < or = 4 cm. Gastroenterology 2004;127:1714–1723
8. Cho YK, Kim JK, Kim MY, Rhim H, Han JK. Systematic review of randomized trials for hepatocellular carcinoma treated with percutaneous ablation therapy. Hepatology 2009;49:453–459
9. Kasugai H, Osaki Y, Oka H, Kudo M, Seki T, Osaka Liver Cancer Study Group. Severe complications of radiofrequency ablation therapy for hepatocellular carcinoma: an analysis of 3891 ablations in 2614 patients. Oncology 2007;72:S72–S75
10. Takeuchi H, Arata T, Takehara K, Shigeyasu K, Kanazawa T, Murata H, et al. A patient who developed diaphragmatic hernia one year after percutaneous radiofrequency ablation for hepatocellular carcinoma. Kanzo 2007;48:458–462
11. Tomonaga C, Kawano A, Taguchi Y, Matsunaga T, Maruyama T, Toyoshima S, et al. Two cases of diaphragmatic hernia following percutaneous radiofrequency ablation of hepatocellular carcinoma. Kanzo 2007;48:529–537
12. Kanai T, Hirohashi S, Upton MP, Noguchi M, Kishi K, Makuuchi M, et al. Pathology of small hepatocellular carcinoma. A proposal for a new gross classification. Cancer 1987;60:810–819
13. Nakashima O, Sugihara S, Kage M, Kojiro M. Pathomorphologic characteristics of small hepatocellular carcinoma: a special reference to small hepatocellular carcinoma with indistinct margins. Hepatology 1995;22:101–105
14. Kojiro M, Nakashima O. Histopathologic evaluation of hepatocellular carcinoma with special reference to small early stage tumors. Semin Liver Dis 1999;19:287–296
15. Kondo Y, Niwa Y, Akikusa B, Takazawa H, Okabayashi A. A histopathologic study of early hepatocellular carcinoma. Cancer 1983;52:687–692
16. Nakashima T, Kojiro M. Hepatocellular Carcinoma: An Atlas of its Pathology. Tokyo: Springer-Verlag; 1987
17. Vilana R, Bruix J, Bru C, Ayuso C, Sole M, Rodes J. Tumor size determines the efficacy of percutaneous ethanol injection for the treatment of small hepatocellular carcinoma. Hepatology 1992;16:353–357
18. Kojiro M. The evolution of pathologic features of hepatocellular carcinoma. In Tabor E, editor. Viruses and Liver Cancer. Amsterdam: Elsevier; 2002. 113–122
19. Kojiro M. Pathology of Hepatocellular Carcinoma. Oxford: Blackwell; 2006. 39–49
20. Taniguchi M, Kim SR, Imoto S, Ikawa H, Ando K, Mita K, et al. Long-term outcome of percutaneous ethanol injection therapy for minimum-sized hepatocellular carcinoma. World J Gastroenterol 2008;14:1997–2002

Value of Liver Parenchymal Phase Contrast-Enhanced Sonography to Diagnose Premalignant and Borderline Lesions and Overt Hepatocellular Carcinoma

Tatsuo Inoue[1]
Masatoshi Kudo[1]
Osamu Maenishi[2]
Mina Komuta[3]
Osamu Nakashima[3]
Masamichi Kojiro[3]
Kiyoshi Maekawa[4]

OBJECTIVE. The objective of our study was to investigate whether liver parenchymal phase contrast-enhanced sonography can provide additional information for assessing histologic grades of hepatocellular carcinoma (HCC).

SUBJECTS AND METHODS. Contrast-enhanced sonography using Levovist of 50 hepatic nodules was performed. The vascular and liver parenchymal perfusion patterns were evaluated. The sensitivity, specificity, and accuracy of the histologic diagnosis of the tumors using vascular phase imaging only and systematically combined vascular phase imaging with liver parenchymal phase imaging were calculated. We also performed histologic examination and immunostaining for the detection of Kupffer cells and calculated the Kupffer cell count in the tumorous tissue relative to that in the nontumorous tissue (Kupffer cell ratio) and quantitatively evaluated the relationship between the Kupffer cell ratio and the perfusion patterns seen on liver parenchymal phase imaging.

RESULTS. The specificity and accuracy of contrast-enhanced sonography in the diagnosis of dysplastic nodules and of moderately and poorly differentiated HCCs were improved by adding liver parenchymal phase imaging (dysplastic nodules, 74% and 78% vs 83% and 86%, respectively; moderately and poorly differentiated HCCs, 74% and 86% vs 85% and 92%). The diagnostic accuracy of contrast-enhanced sonography for dysplastic nodules showed a trend of improvement with the addition of liver parenchymal phase imaging ($p = 0.07$). Kupffer cell ratios for tumors that showed hypoperfusion during the liver parenchymal phase were significantly lower than those for tumors showing isoperfusion ($p < 0.05$).

CONCLUSION. Adding liver parenchymal phase imaging to contrast-enhanced sonography protocols may yield additional information that can be used to assess histologic grades of tumor and that leads to an improvement in the differential diagnosis of nodular lesions associated with the cirrhotic liver. Further case studies are required in larger numbers of patients for a longer follow-up period.

Keywords: cirrhotic liver, contrast-enhanced sonography, dysplastic nodules, hepatocellular carcinoma, Kupffer cells, liver parenchymal phase imaging

DOI:10.2214/AJR.07.3282

Received October 10, 2007; accepted after revision September 6, 2008.

[1]Division of Gastroenterology and Hepatology, Department of Internal Medicine, Kinki University School of Medicine, 377-2, Ohno-Higashi, Osaka-Sayama, Osaka 589-8511, Japan. Address correspondence to M. Kudo (m-kudo@med.kindai.ac.jp).

[2]Department of Pathology, Kinki University School of Medicine, Osaka, Japan.

[3]First Department of Pathology, Kurume University School of Medicine, Fukuoka, Japan.

[4]Abdominal Ultrasound Unit, Kinki University School of Medicine, Osaka, Japan.

AJR 2009; 192:698–705

0361–803X/09/1923–698

Hepatocellular carcinoma (HCC) is one of the most common cancers worldwide and is a major cause of death in patients with cirrhosis. Therefore, it is important to detect and treat HCC at an early stage. Because the histopathologic grade of HCC is a well-established prognostic factor and affects the choice of the initial treatment, precise diagnosis of the histologic grade is essential. Previously, Kupffer cells were thought to be absent in overt HCC tissues, but recently investigators have shown that Kupffer cells exist in well-differentiated and early-stage HCCs [1]. Furthermore, the histologic grade of HCC has been shown to correlate with the number of Kupffer cells present. For example, in cancerous tissues the number of Kupffer cells present was significantly lower than in noncancerous tissues and tended to decrease as the histologic grade of tumor decreased [1].

The microbubble contrast agent SH U 508A (Levovist, Schering) for sonography has improved the ability to detect and characterize the intranodular vascularity of hepatic lesions [2], and vascular phase contrast-enhanced sonography has become an established diagnostic method for hepatic tumors [3–6]. Until now, no study to our knowledge has systematically combined arterial and portal phase imaging with liver parenchymal phase imaging to diagnose premalignant and borderline lesions and HCCs. The purpose of our study, therefore, was to evaluate whether liver parenchymal phase contrast-enhanced sonography

can provide additional information for assessing the histologic grade of HCCs.

Subjects and Methods

Between June 2002 and September 2004, 2,240 patients underwent contrast-enhanced sonography at our institution. Among them, 168 patients had a single hepatic nodule that had not previously been treated, 57 of whom had undergone tumor biopsy or partial hepatectomy. Two patients were excluded from this study because their tumors were located on the deep side of the liver and contrast-enhanced sonography could not detect them. Another five patients who underwent liver biopsy were excluded from this study because a pathologic diagnosis could not be obtained. As a result, 50 consecutive patients who had a single hepatic nodule that was examined histologically were prospectively included in this study.

Thirty-eight patients were men and 12 patients were women, with a median age of 67 years (age range, 51–84 years). Forty-two patients had hepatitis C virus–related cirrhosis, six patients had hepatitis B virus–related cirrhosis, and two had cirrhosis of unknown origin. According to the Child-Pugh classification [7], liver function was categorized as Child-Pugh A in 40 patients, Child-Pugh B in seven, and Child-Pugh C in three. Written informed consent was obtained from all patients. Therefore, patients understood that biopsy of adjacent normal liver was required for research purposes only, and the potential complications arising from this biopsy were explained to patients before they were asked to provide informed consent. This study was approved by the institutional review board of the Kinki University School of Medicine.

Study Design

We analyzed three parameters. First, we classified the perfusion patterns of each tumor on contrast-enhanced sonography during the arterial and portal phases and during the liver parenchymal phase. Second, we calculated the sensitivity, specificity, and accuracy of diagnostic methods that use arterial and portal phase imaging only and those that use a combination of arterial and portal phase imaging with liver parenchymal phase imaging. Third, we compared the Kupffer cell count ratios of the tumors between groups that were classified according to perfusion patterns in the liver parenchymal phase. Levovist that is taken up by the reticuloendothelial system in liver parenchyma is considered to be an echo source on liver parenchymal phase imaging. Therefore, liver parenchymal phase imaging of the tumor might show different findings according to the number of Kupffer cells detected, so it is important to standardize the relative uptake ratio to the tumors compared with liver parenchyma. Thus, we counted the Kupffer cell ratios as follows: number of Kupffer cells in the tumor divided by that in the liver parenchyma.

Diagnosis of HCCs and Dysplastic Nodules

In the 50 patients, we detected 50 nodules with a median diameter of 2.7 cm (range, 1.2–5.2 cm) on sonography. All 50 tumors were histologically diagnosed as either dysplastic nodules or HCCs in a blinded manner by four pathologists according to the histologic criteria of the International Working Party [8]. Liver specimens from 43 patients were obtained by 18-gauge needle core biopsy (Majima needle, Top). In each case, at least two specimens were obtained from the nodular lesion and one specimen from the adjacent nonnodular area. Additional specimens from tumors and nontumors were obtained by surgical operation from seven patients who underwent partial hepatectomy.

Contrast-Enhanced Sonography

A sonography unit with a wideband convex and sector transducer (Aplio, Toshiba Medical Systems) was used for all sonographic studies. To find an adequate scanning plane to clearly show the tumors and adjacent liver, fundamental B-mode imaging was used before injection of the contrast agent. Thereafter, the advanced dynamic flow mode was performed with a mechanical index of 1.4. Different frame rates are used: 5 frames per second in the early arterial phase and 0.25 frame per second in the late and liver parenchymal phases. The focus point was set with one point at the deepest edge of the lesion. The advanced dynamic flow procedure was observed in three phases: the arterial phase, from 10 to 60 seconds after microbubble administration; portal phase, from 1 to 2 minutes after microbubble administration; and liver parenchymal phase, 10 minutes after the second injection of microbubbles.

A bolus of 3 mL (300 mg/mL) of Levovist was then injected by hand via a 20-gauge IV cannula at a rate of approximately 1 mL/s, followed by a 10-mL normal saline flush. To diminish motion artifacts and avoid losing sight of the target tumor, sonographers asked patients to hold their breath beginning 10 seconds after microbubble administration (when the first enhanced signal appeared in the liver). Real-time imaging was then observed for 20–30 seconds to detect the pattern of the supplying blood vessels in the arterial phase and for 10 seconds in the portal phase after the arterial phase observation. After vascular phase imaging was observed, an additional 4 mL (300 mg/mL) of microbubbles was injected.

Ten minutes after the second injection of microbubbles, perfusion of the nodules and adjacent liver was examined using liver parenchymal phase imaging. A gradual change in the scanning plane was needed to observe the entire nodule. The cine loop memory was recalled, and still images were saved in magneto-optic disks. All of these contrast-enhanced studies were reviewed, and the intranodular hemodynamics were evaluated, as described in the Results section, by three blinded reviewers who were unaware of the findings from the other imaging techniques and of the pathologic and clinical data. In case of discrepancy, the reviewers assessed the saved images together and reevaluated their findings to reach an agreement.

Each phase image was classified as follows: hypervascular or not in the arterial phase; hyperperfusion, isoperfusion, or hypoperfusion in the portal phase; and isoperfusion or hypoperfusion in the liver parenchymal phase. Type 1 nodules were classified as those that exhibited intranodular vessels in the arterial phase. Nodules that did not exhibit intranodular vessels in the arterial phase but showed hypoperfusion or isoperfusion in the portal phase were classified as type 2 or type 3, respectively.

The type 1 group was further subdivided into type 1a and type 1b nodules according to the liver parenchymal perfusion pattern. The type 1 nodules that had perfusion defects in the liver parenchymal phase were classified as type 1a and those that showed isoperfusion were classified as type 1b. The type 3 group was further subdivided into type 3a and type 3b nodules according to the liver parenchymal perfusion pattern. The type 3 nodules that had perfusion defects in the liver parenchymal phase were classified as type 3a and those that showed isoperfusion were classified as type 3b.

After we classified the vascular and perfusion patterns of the tumors, we calculated the sensitivity, specificity, and accuracy of the diagnostic method that used vascular phase imaging only and the diagnostic method that used a combination of arterial and portal phase imaging and liver parenchymal phase imaging.

Immunohistochemistry of Kupffer Cells

In addition to routine staining with H and E for the morphologic study, immunostaining for Kupffer cells using the indirect immunoperoxidase method was performed on representative formalin-fixed and paraffin-embedded tissue sections from each tumor and from control areas. Cells that immunostained positively with an antihuman macrophage antibody (anti-CD68 [PGM1] antibody [Dakopatts]) and that had a stellate or spindle shape were considered to be